

Dedicated to Rolf Hagedorn

STRANGENESS and QUARK-GLUON PLASMA

what has been learned so far, where do we go?

with Jean Letessier

Department of Physics, University of ARIZONA, Tucson
and
LPTHE-University Paris 7-Jussieu

SQM2003, Atlantic City, North Carolina, March 12, 2003

- [I] Strangeness in HI-collisions
a retrospective (p2-11)
- [II] Statistical Hadronization
Analysis method of particle yields (and distributions)(p12-19)
- [III] Compare SPS with RHIC: Strangeness
per baryon, per entropy, per quark pairs (p20-27)
- [IV] Quark-gluon QCD matter
and supercooling/sudden breakup (p28-37)
- [V] How strangeness/charm is made
and how it evolves (p38-43)

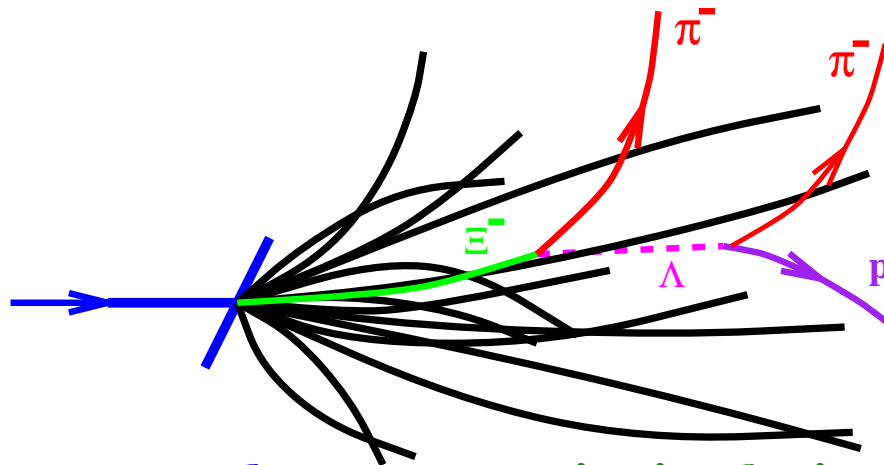
Strangeness – a popular QGP diagnostic tool

EXPERIMENTAL REASONS

- There are **many** strange particles allowing to study **different physics questions** ($q = u, d$):

$$\phi(s\bar{s}), \quad K(q\bar{s}), \quad \bar{K}(\bar{q}s), \quad \Lambda(qqs), \quad \bar{\Lambda}(\bar{q}\bar{q}\bar{s}), \\ \Xi(qss), \quad \bar{\Xi}(\bar{q}\bar{s}\bar{s}), \quad \Omega(sss), \quad \bar{\Omega}(\bar{s}\bar{s}\bar{s})$$

- Strange hadrons are subject to a **self analyzing decay** within a **few cm** from the point of production;



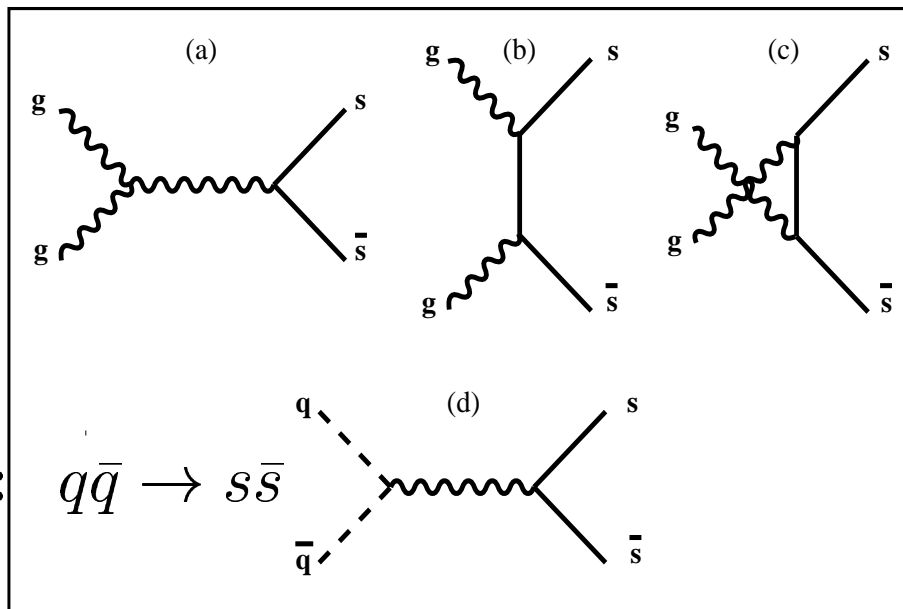
- Production rates hence **statistical significance is high**;

THEORETICAL CONSIDERATIONS

- production of strangeness in gluon fusion $GG \rightarrow s\bar{s}$
strangeness linked to gluons from QGP;

dominant processes:
 $GG \rightarrow s\bar{s}$

10–15% of total rate:



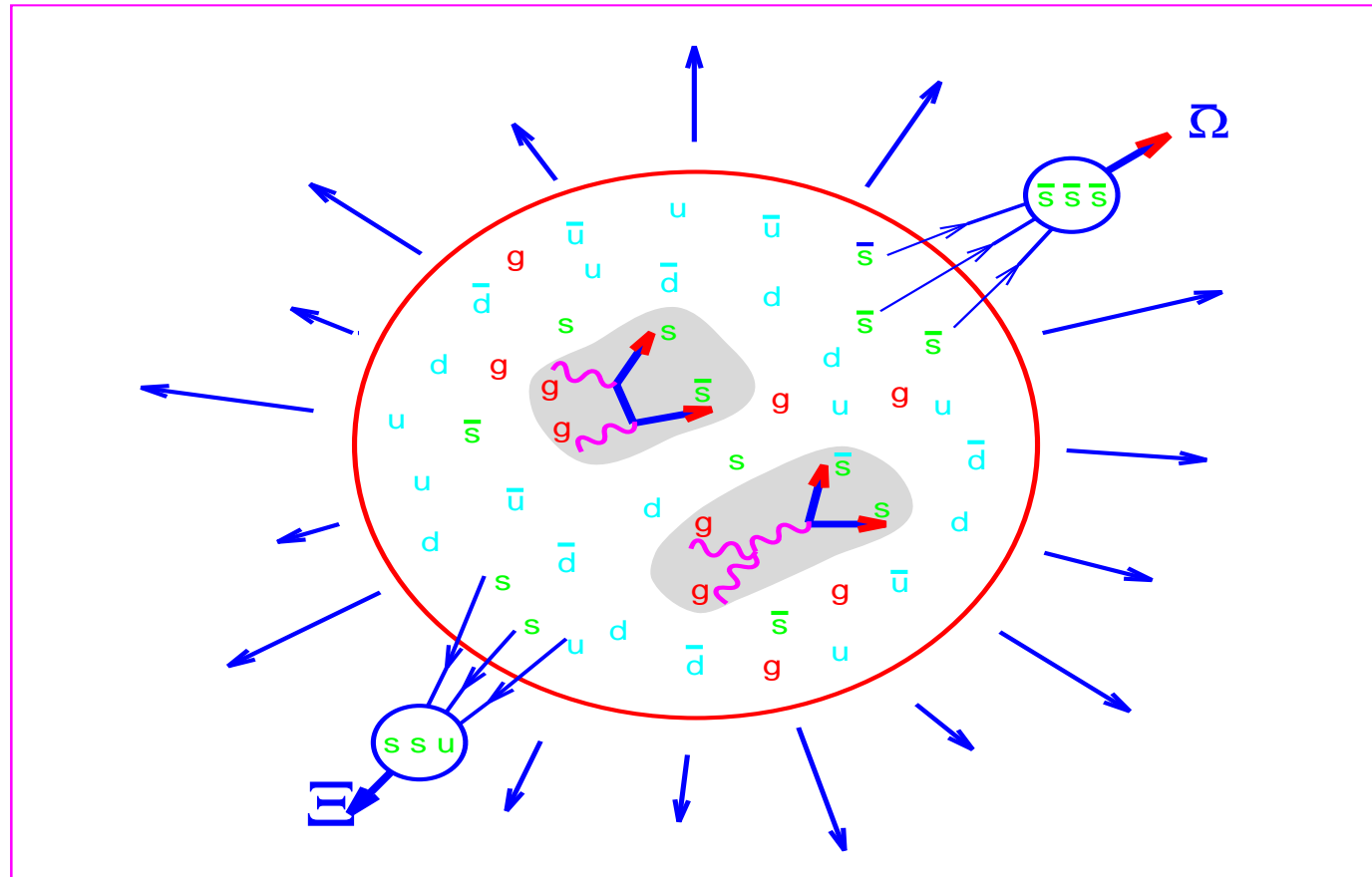
- coincidence of scales:

$$\boxed{m_s \simeq T_c} \rightarrow \boxed{\tau_s \simeq \tau_{\text{QGP}}} \rightarrow$$

strangeness a clock for reaction

- Often $\bar{s} > \bar{q}$ \rightarrow strange antibaryon enhancement and at RHIC also (anti)hyperon dominance of (anti)baryons.

'CROSS-TALK' HADRON FORMATION MECHANISM IN QGP

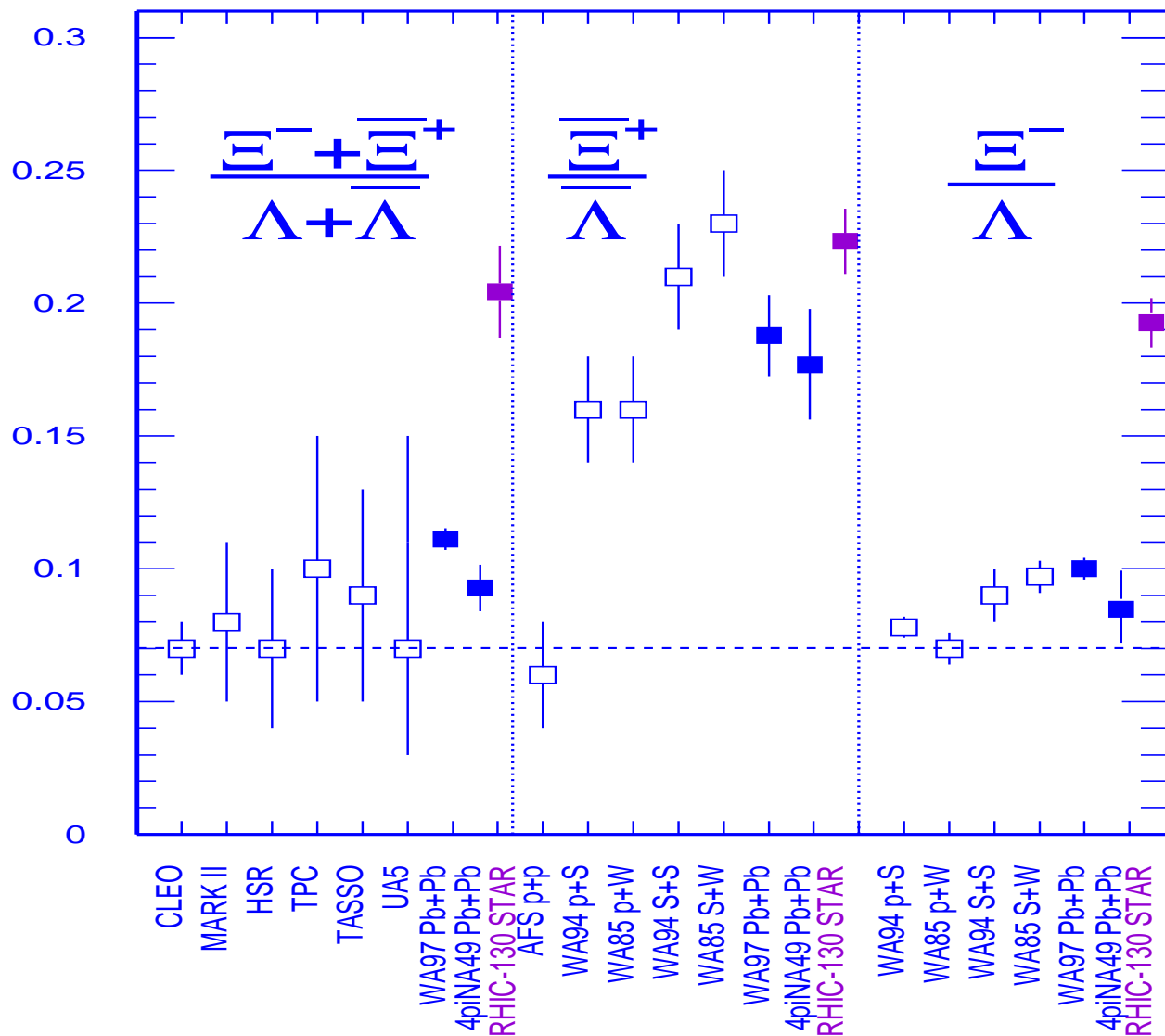


Formation of complex rarely produced multi strange (anti)particles form QGP enabled by 'cross talk' between quarks made in different microscopic reactions = deconfinement. Enhancement of strange antibaryons progressing with strangeness content.

Retrospective: Strangeness Discoveries

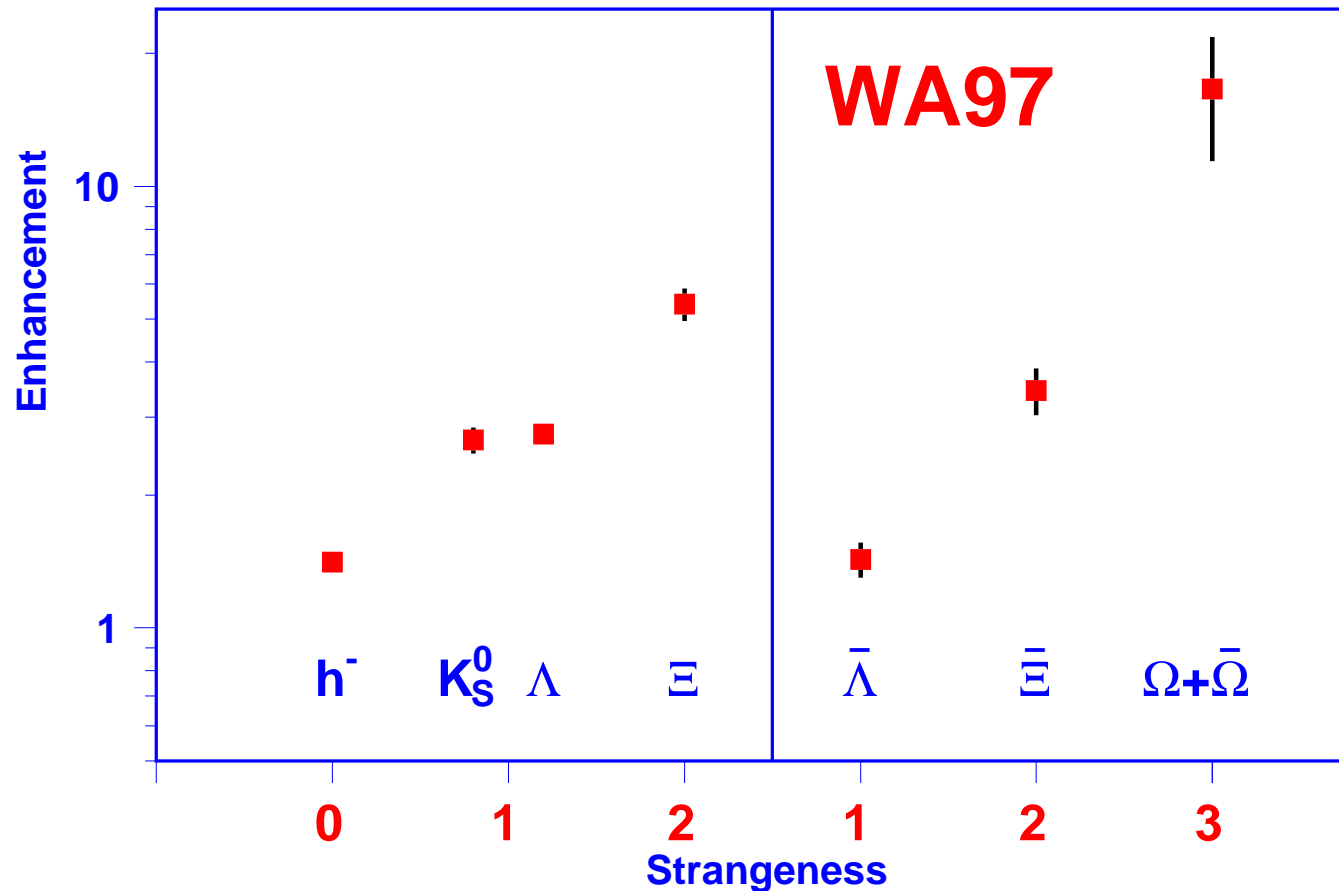
MULTISTRANGE ANTI-HYPERON RATIOS:

A predicted QGP signature



MULTISTRANGE (ANTI)HYPERON ENHANCEMENT

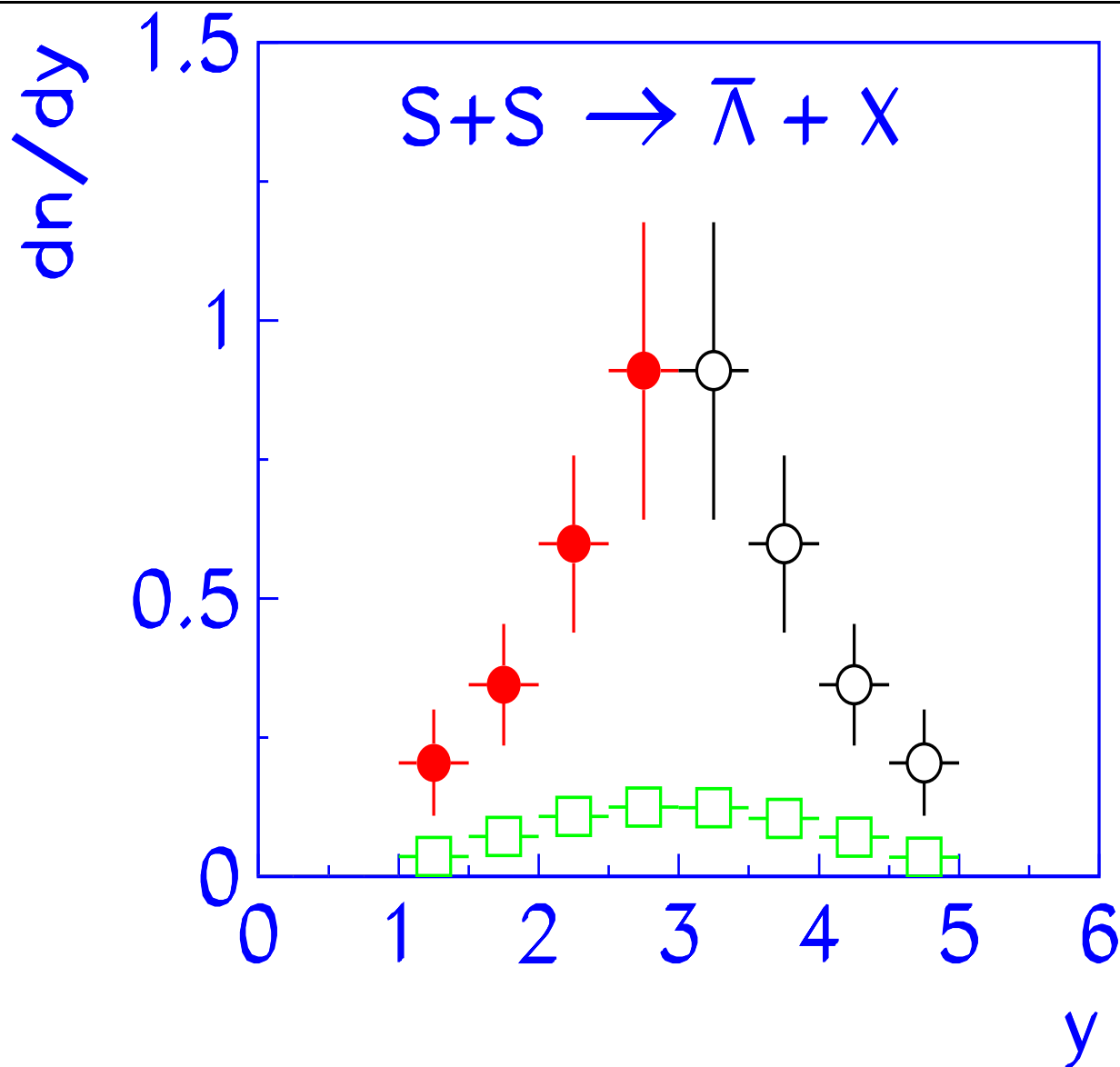
A predicted QGP signature



Prediction of enhancement GROWTH with
a) strangeness b) antiquark content.

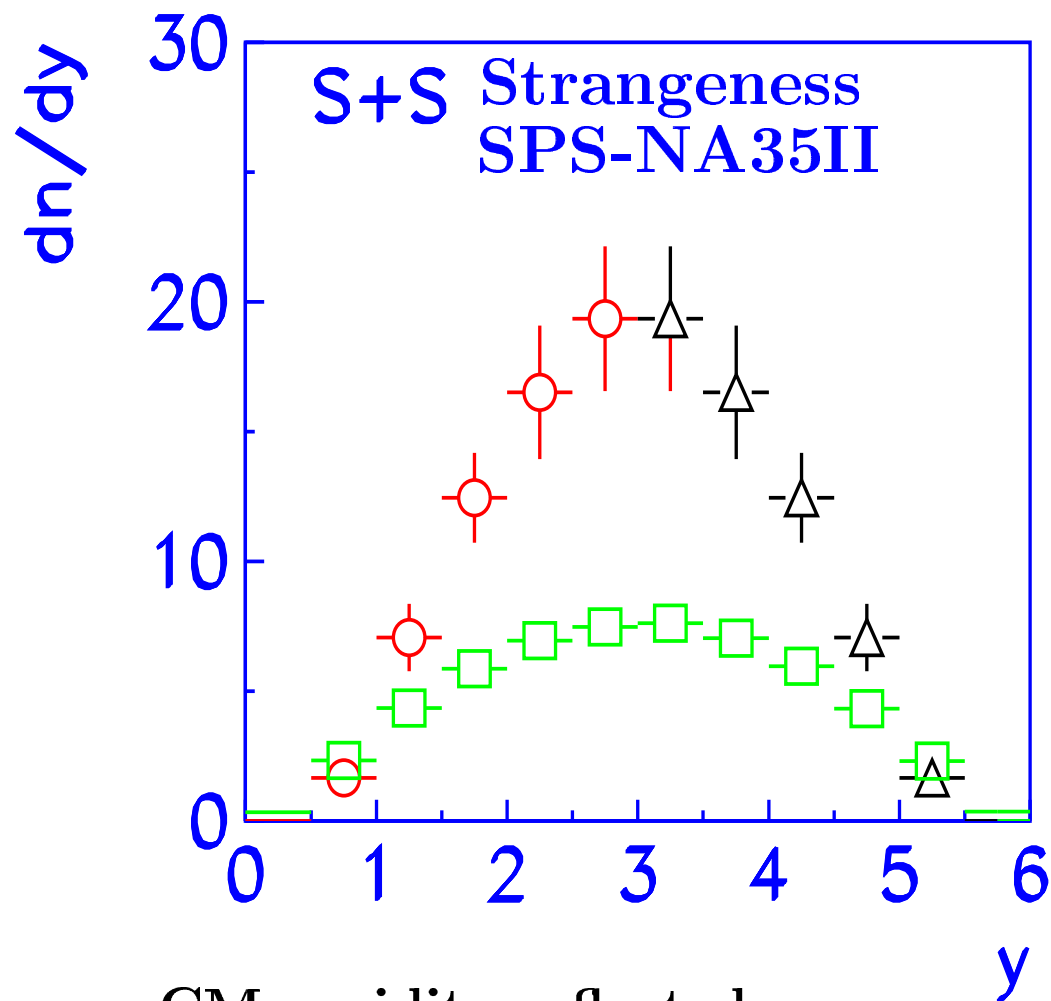
Enhancement with respect to the yield in p-Be collisions, scaled up with the number of 'wounded' nucleons.

Antibaryon excess IS at central CM rapidity



NA35II EXCESS $\bar{\Lambda}$ emitted from a central well localized source.
Background (squares) from multiplicity scaled NN reactions
forward (open circles) points: reflection at CM rapidity

Strangeness Enhancement at central CM rapidity



CM-rapidity reflected

1.6 Λ + 1.6 $\bar{\Lambda}$ + 4 K_S 200 A GeV S on S

multiplicity scaled 200 A GeV p on p

High m_{\perp} slope universality

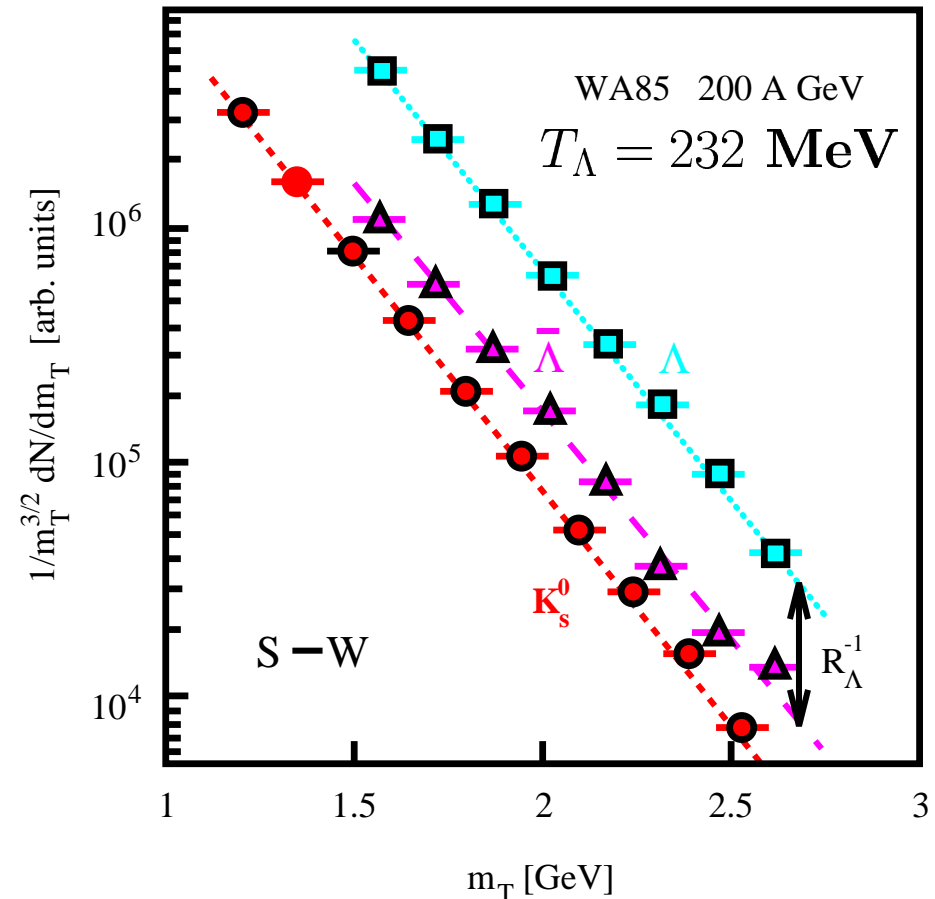
Discovered in S-induced collisions, pronounced in Pb-Pb Interactions.

Why is the slope of baryons and antibaryons precisely the same?

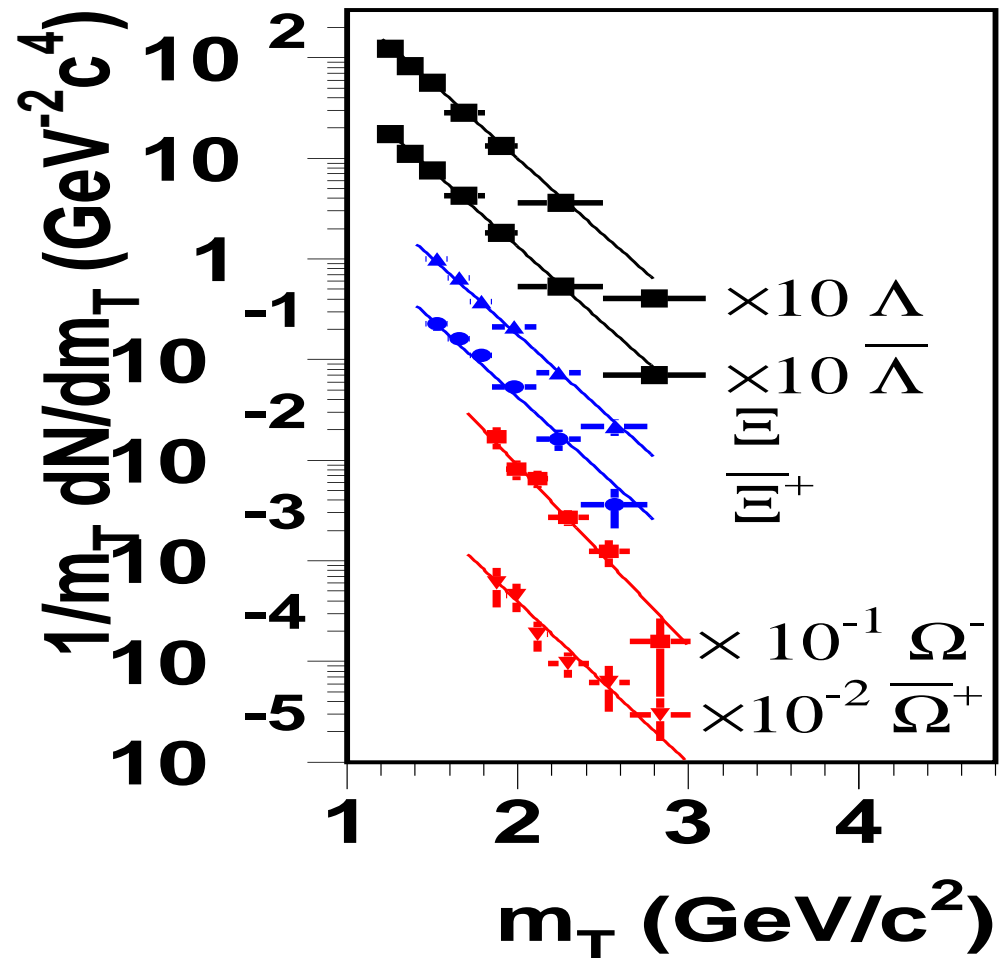
Why is the slope of different hyperons in same m_t range the same?

Analysis+Hypothesis 1991:
QGP quarks coalescing in SUDDEN hadronization

This allowed the study of ratios of particles measured only in a fraction of phase space



WA97	T_{\perp}^{Pb} [MeV]
T^{K^0}	230 ± 2
T^{Λ}	289 ± 3
$T^{\bar{\Lambda}}$	287 ± 4
T^{Ξ}	286 ± 9
$T^{\bar{\Xi}}$	284 ± 17
$T^{\Omega+\bar{\Omega}}$	251 ± 19



Λ within 1% of $\bar{\Lambda}$

Kaon – hyperon difference: **EXPLOSIVE FLOW** effect

Difference between $\Omega + \bar{\Omega}$: excess of low p_{\perp} particles (?) fluctuation

WHEN FLOW MORE EXPLOSIVE (RHIC) MORE CAREFUL ANALYSIS OF m_{\perp} SPECTRA REQUIRED (G. Torrieri, Sunday session#4, 15:10)

Same slopes of baryons and antibaryons, different hyperons:

1) same production process, 2) **NO KINETIC REEQUILIBRATION,**

3) some effect of resonance decays

→STATISTICAL HADRONIZATION:

WHAT IS IT, AND HOW WE ARE LOOKING FOR IT

Quarks and gluons constrained by external 'frozen color vacuum', propagating over a volume much larger than nucleon size.

We expect to encounter a phase transformation between confined and deconfined phases, this is NOT an equilibrium environment.

There are several stepping stones:

- 1) Observing hadrons requires functioning model of hadronization,
- 2) We need to understand QGP equilibrium properties and
- 3) Understand how to adapt these to the dynamical RHIC case,
- 4) Return to check strangeness production and evolution into hadrons.

We need to pursue global, systematic and physics-consistent understanding of all experimental results. Where we are not able (yet) to compute, a in principle interpretation should be available.

OUTLOOK: When reaching a consensus about discoveries, we keep in mind that there is a difference between: verified predictions, accompanied by expected global behavior, and inventive post-dictions, limited in scope to punctual experimental data interpretation.

II STATISTICAL HADRONIZATION

Objective: Obtain a valid description of particle production yields and spectra in order to understand both intensive (T_h, \dots), and extensive (energy, baryon, strangeness, entropy content) properties of the fireball.

This requires the knowledge of the phase space of hadronic particles in great precision.

Method: Attend

Primary hypothesis of statistical hadronization

Within a ‘family’, particle yields with same valance quark content are in relation to each other thermally equilibrated, e.g. the relative yield of $\Delta(1230)(qqq)$ and $N(qqq)$ completely controlled by ratios $m_N/T, m_\Delta/T$ e.g statistical weights (**Hagedorn**):

$$\frac{n_\Delta}{n_N} = \frac{g_\Delta(m_\Delta/T)^{3/2}e^{-m_\Delta/T}}{g_N(m_N/T)^{3/2}e^{-m_N/T}}$$

Comprehensive test still outstanding.

Chemical Potentials and fugacities

particle fugacity: $\Upsilon_i \equiv e^{\sigma_i/T} \iff \sigma_i$ particle 'i' chemical potential

Example of NUCLEONS:

two particles $N, \bar{N} \rightarrow$ two chemical factors, convenient choice:

$$\sigma_N \equiv \mu_b + T \ln \gamma_N, \quad \sigma_{\bar{N}} \equiv -\mu_b + T \ln \gamma_N;$$

$$\Upsilon_N = \gamma_N e^{\mu_b/T}, \quad \Upsilon_{\bar{N}} = \gamma_N e^{-\mu_b/T}.$$

The (baryo)chemical potential μ_b , controls the particle difference = **baryon number**. This can be seen looking at the first law of thermodynamics:

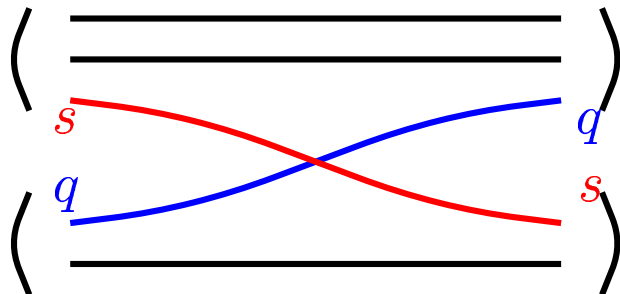
$$\begin{aligned} dE + P dV - T dS &= \sigma_N dN + \sigma_{\bar{N}} d\bar{N} \\ &= \mu_b(dN - d\bar{N}) + T \ln \gamma_N(dN + d\bar{N}). \end{aligned}$$

γ regulates the number of nucleon-antinucleon pairs present.

FOUR QUARKS: $s, \bar{s}, q, \bar{q} \rightarrow$ FOUR CHEMICAL PARAMETERS

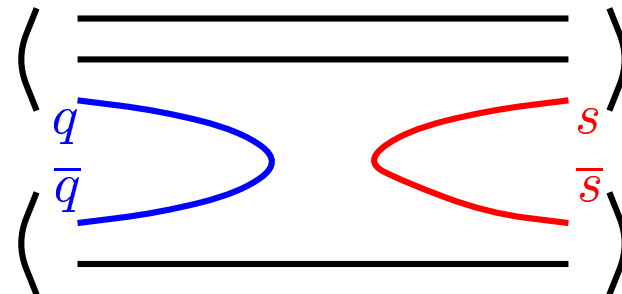
γ_i controls overall abundance of quark ($i = q, s$) pairs	Absolute chemical equilibrium
λ_i controls difference between strange and non-strange quarks ($i = q, s$)	Relative chemical equilibrium

HG-EXAMPLE: redistribution,
Relative chemical equilibrium



EXCHANGE REACTION

production of strangeness
Absolute chemical equilibrium



PRODUCTION REACTION

We imply that locally **thermal** equilibrium is established.
Chemical equilibrium, if present, could be result of fit.

To characterize a particle we follow the valance quark content of a hadron forming a product of factors γ_i , and λ_i , e.g. for $p(uud)$:

$$\Upsilon_{p(uud)} = \gamma_u^2 \gamma_d \lambda_u^2 \lambda_d, \quad \Upsilon_{\bar{p}(\bar{u} \bar{u} \bar{d})} = \gamma_u^2 \gamma_d \lambda_u^{-2} \lambda_d^{-1},$$

note that:

$$\lambda_i = e^{\mu_i/T}, \quad \mu_q = \frac{1}{2}(\mu_u + \mu_d), \quad \lambda_q^2 = \lambda_u \lambda_d \quad \lambda_b = \lambda_q^3.$$

This implies relations between quark and hadron potential:

$$\mu_b = 3\mu_q \quad \mu_s = \frac{1}{3}\mu_b - \mu_S, \quad \lambda_s = \frac{\lambda_q}{\lambda_S},$$

Remember: **NEGATIVE S-strangeness in s-hadrons.** e.g. for $\Lambda(uds)$:

$$\Upsilon_{\Lambda} = \gamma_u \gamma_d \gamma_s e^{(\mu_u + \mu_d + \mu_s)/T} = \gamma_u \gamma_d \gamma_s e^{(\mu_b - \mu_S)/T},$$

Phase space density is:

$$\frac{d^6 N_i}{d^3 p d^3 x} = g_i \frac{\Upsilon_i}{(2\pi)^3} e^{-E_i/T}, \quad \frac{d^6 N_i^{\text{F/B}}}{d^3 p d^3 x} = \frac{g_i}{(2\pi)^3} \frac{1}{\Upsilon_i^{-1} e^{E_i/T} \pm 1}, \quad \Upsilon_i^{\text{bosons}} \leq e^{m_i/T},$$

HOW DOES STATISTICAL HADRONIZATION WORK?

The 4π particle yields the particle abundance is proportional to phase space integrals – no influence of matter flow dynamics.

$$\frac{N_\pi}{V} = C g_\pi \int \frac{d^3p}{(2\pi)^3} \frac{1}{\gamma_q^{-2} e^{\sqrt{m_\pi^2 + p^2}/T} - 1}, \quad \gamma_q^2 < e^{m_\pi/T} \simeq (1.6)^2$$

$$\frac{N}{V} = C g_N \int \frac{d^3p}{(2\pi)^3} \frac{1}{1 + \gamma_q^{-3} \lambda_q^{-3} e^{E/T}} \quad \bar{N} = C g_N \int \frac{d^3p}{(2\pi)^3} \frac{1}{1 + \gamma_q^{-3} \lambda_q^{+3} e^{E/T}}$$

Integrals easily computed. Proportionality constant C NOT A VOLUME for a dynamically evolving system.

Consideration valid at RHIC/LHC with Bjorken- y -scaling equivalent infinite series of fireballs at all rapidities (Hagedorn).

EXAMPLE: RATIOS OF PARTICLE YIELDS

$$R_\Lambda = \frac{\bar{\Lambda}}{\Lambda} = \frac{\bar{\Lambda} + \bar{\Sigma}^0 + \bar{\Sigma}^* + \dots}{\Lambda + \Sigma^0 + \Sigma^* + \dots} = \frac{\bar{s}\bar{q}\bar{q}}{sqq} = \lambda_s^{-2}\lambda_q^{-4} = e^{2\mu_s/T}e^{-2\mu_b/T}.$$

$$R_\Xi = \frac{\bar{\Xi}^-}{\Xi^-} = \frac{\bar{\Xi}^- + \bar{\Xi}^* + \dots}{\Xi^- + \Xi^* + \dots} = \frac{\bar{s}\bar{s}\bar{q}}{ssq} = \lambda_s^{-4}\lambda_q^{-2} = e^{4\mu_s/T}e^{-2\mu_b/T}.$$

In combination we have here an estimates of (baryon) chemical potential (Peter Koch et al, PLB123(1983)151),

Sensitivity to occupancy factors γ_i derives from comparison of hadron yields with differing q, s quark content e.g.:

$$\frac{\Xi^-(dss)}{\Lambda(dds)} \propto \frac{\gamma_d\gamma_s^2}{\gamma_d^2\gamma_s} \frac{g_\Xi\lambda_d\lambda_s^2}{g_\Lambda\lambda_d^2\lambda_s}.$$

note: $\gamma_q^2 \equiv \gamma_u\gamma_d$, $\gamma_u \simeq \gamma_d$

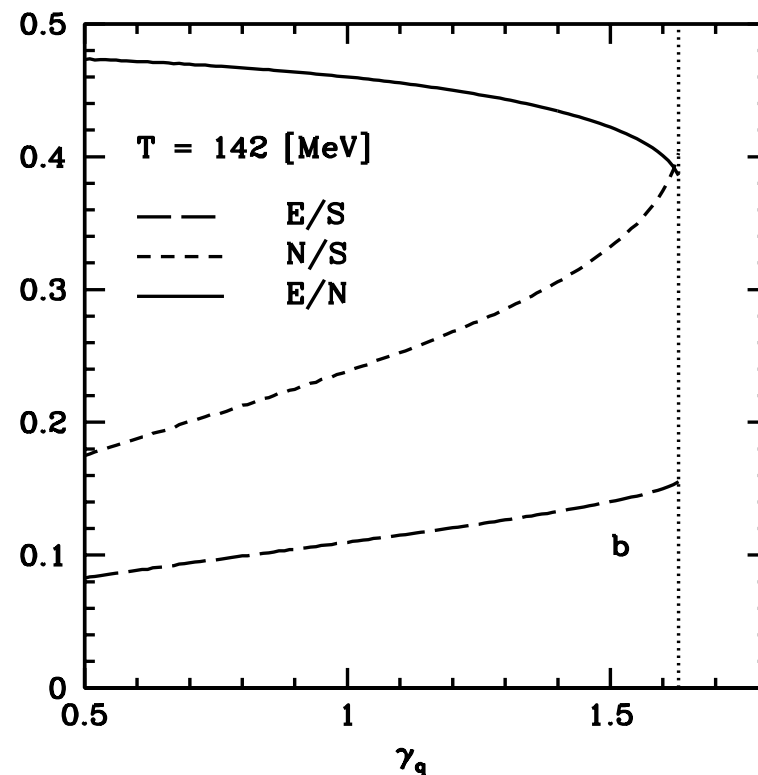
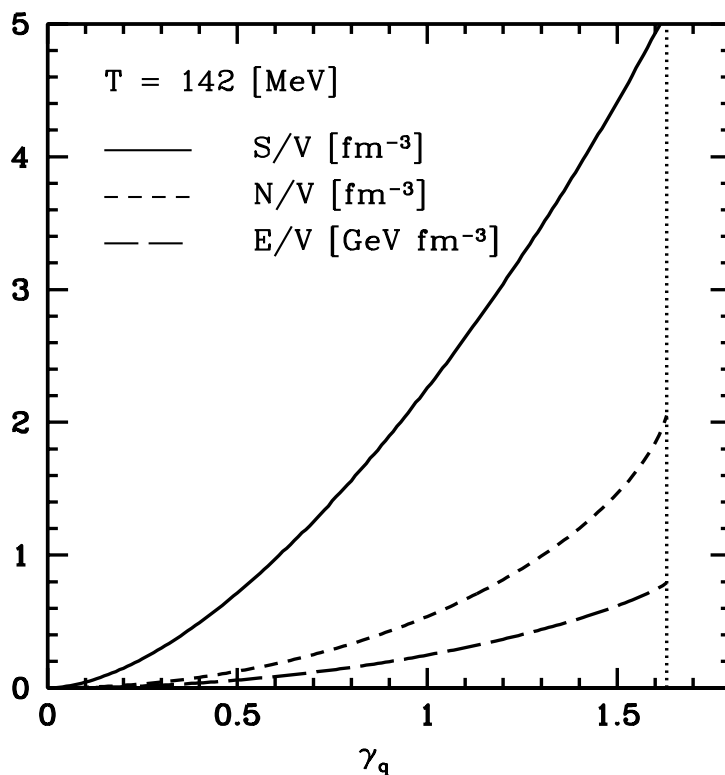
SPECIAL ROLE OF $\gamma_q^2 \rightarrow e^{m_\pi/T}$

Maximization of entropy density in pion: gas.

$$E_\pi = \sqrt{m_\pi^2 + p^2}$$

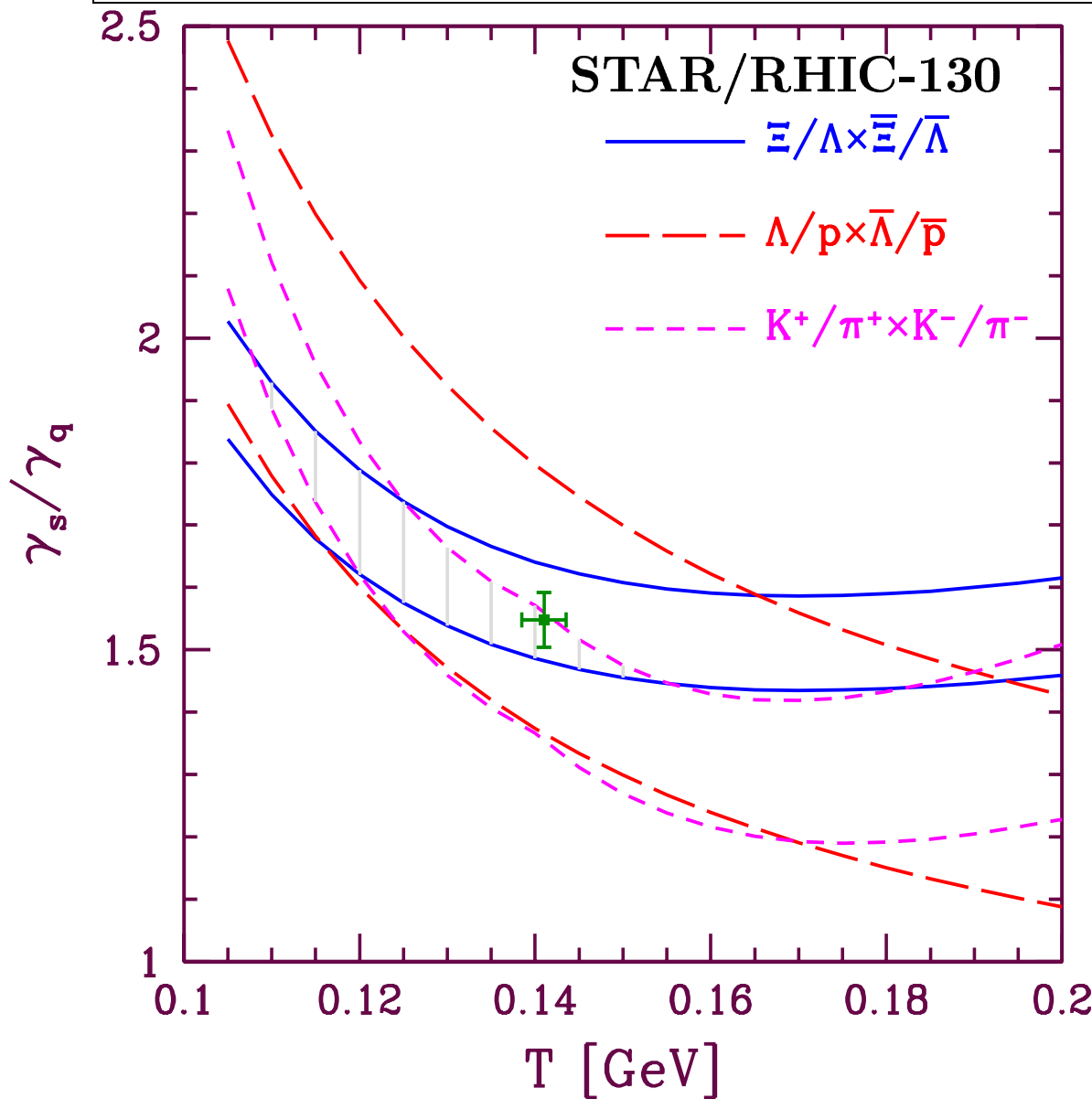
$$S_{B,F} = \int \frac{d^3p d^3x}{(2\pi\hbar)^3} [\pm(1 \pm f) \ln(1 \pm f) - f \ln f], \quad f_\pi(E) = \frac{1}{\gamma_q^{-2} e^{E_\pi/T} - 1}.$$

Pion gas properties: N -particle, E -energy, S -entropy, V -volume as function of γ_q .



A way to 'consume' excess of QGP entropy

STRANGENESS PHASE SPACE OVERPOPULATED at RHIC



In some particle ratios all chemical factors but the ratio of final state phase space occupancies γ_s/γ_q cancel.

Equilibrium population CONVINCINGLY excluded.

CROSS: best fit to all data, Note:

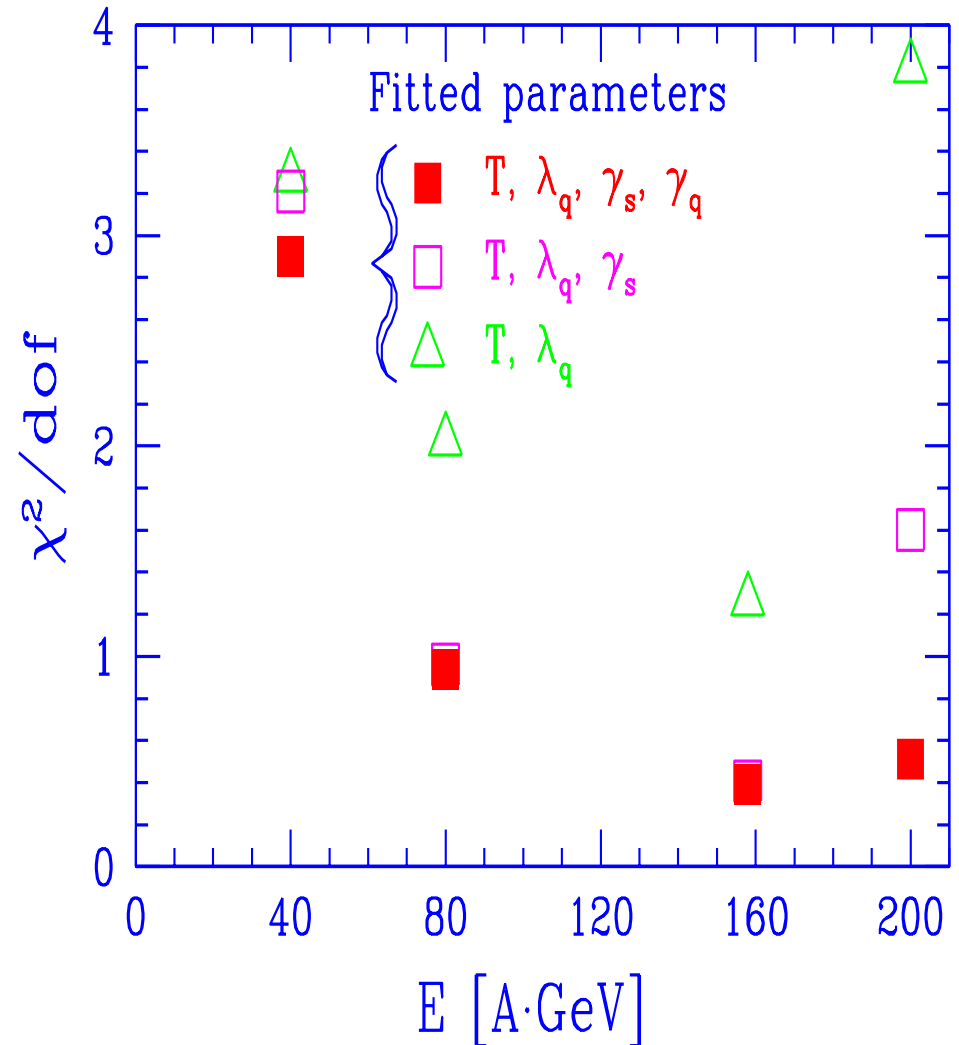
OUTLOOK: Use particle distributions to determine matter dynamics (flow), and hadronization hyper surface.

III COMPARE SPS WITH RHIC

METHOD OF COMPARISON

Apply statistical hadronization code to a comparable sample of particles for Pb-Pb NA49¹ 40A GeV, 80A GeV, WA97 and NA49 158A GeV, and WA85 S-W 200A GeV results. Good statistical significance found allowing chemical non equilibrium except at 40A GeV, where non-statistical production mechanism could be visible (?), e.g. for rarely produced $\bar{\Lambda}, \bar{\Phi}$. Show results along with QM2002 STAR/PHOENIX RHIC130 analysis.

¹We thank M. Gazdzicki for a very useful compilation of NA49 results



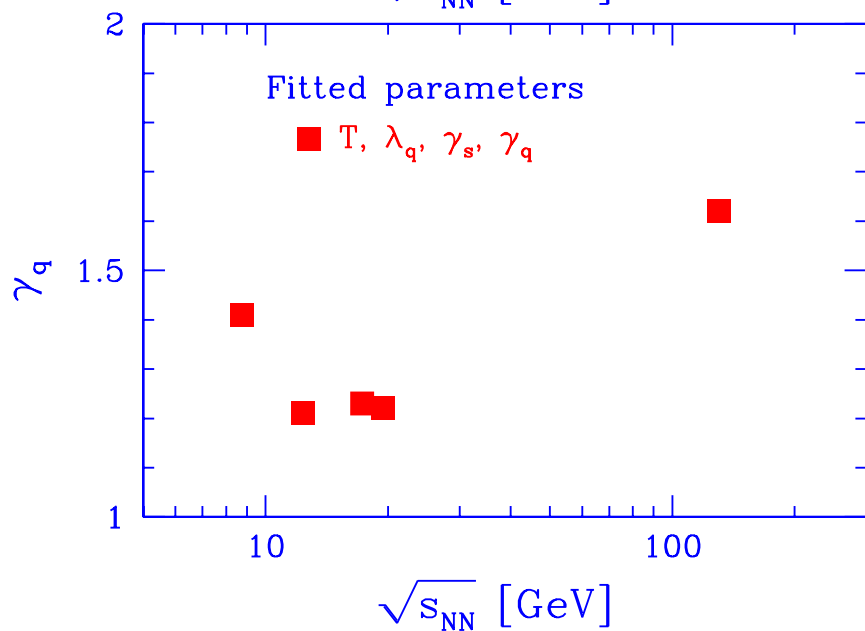
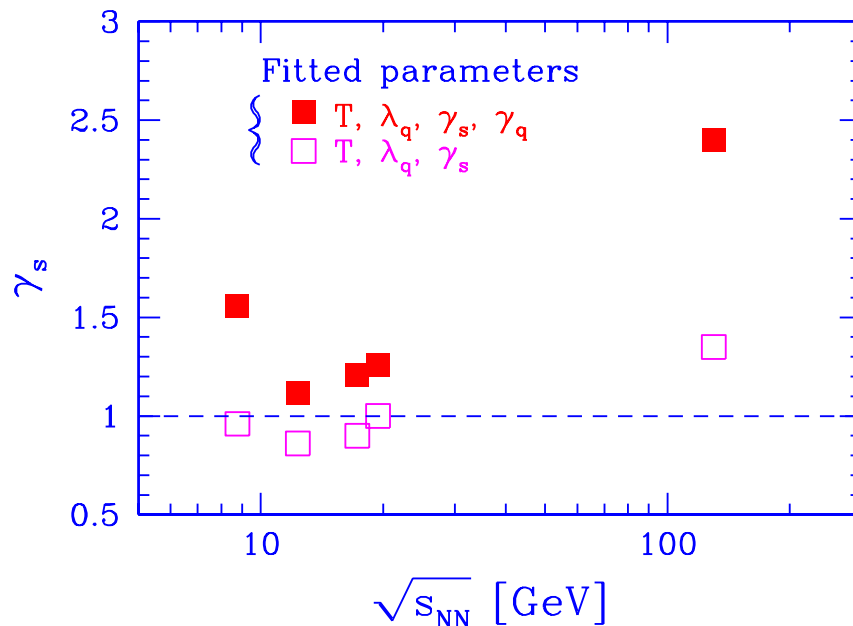
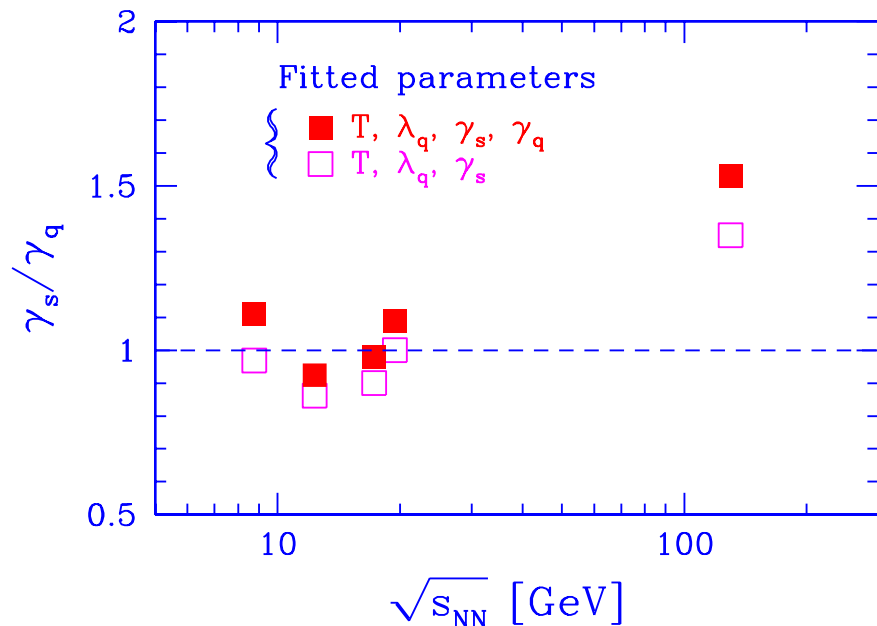
EVALUATE EXTENSIVE PROPERTIES OF THE FIREBALL

Given fitted set of statistical parameters (T, μ_i, γ_i) which characterize the phase space we can evaluate, up to a common normalization constant, the energy, entropy, baryon number, strangeness, etc. content of all produced particles.

EXAMPLE: RHIC-130

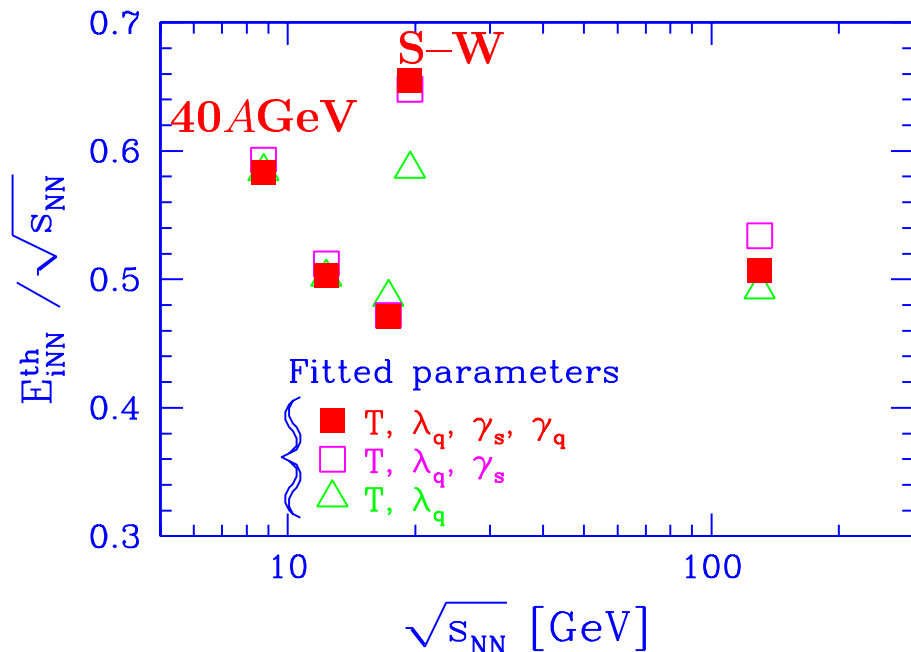
	100% $\Xi \rightarrow Y$ 40% $Y \rightarrow N$	40% $\Xi \rightarrow Y$ 40% $Y \rightarrow N$	40% $\Xi \rightarrow Y$ 40% $Y \rightarrow N$
T	140.1 ± 1.1	142.3 ± 1.2	164.3 ± 2.2
λ_q	1.070 ± 0.008	1.0685 ± 0.008	1.065 ± 0.008
λ_s	1.0136^*	1.0216^*	1.0196^*
γ_q^{HG}	1.64^*	1.63^*	1^*
$\gamma_s^{\text{HG}} / \gamma_q^{\text{HG}}$	1.54 ± 0.04	1.54 ± 0.04	1^*
μ_b [MeV]	28.4	28.3	31.0
μ_s [MeV]	6.1	6.4	7.1
s/b	9.75	9.7	7.2
E/b [GeV]	35.0	34.6	34.8
S/b	234.8	230.5	245.7
E/S [MeV]	148.9	150.9	141.5
χ^2/dof	$7.1/(19 - 3)$	$19/(19 - 3)$	$177.2/(19 - 2)$
	non-equilibrium		equilibrium

Hadronization phase space occupancy



Allowing $\gamma_q^{\text{HG}} \neq 1$ fits are statistically significant. We find, most clearly so at RHIC, that hadronization is accompanied by $\gamma_s^{\text{HG}} > 1$. Recall: we used NA49 results for $K, \bar{K}, \Lambda, \bar{\Lambda}, \phi$ at 40,80,160 AGeV and find at top SPS energy using this data sample a $\gamma_q^{\text{HG}} > 1$, but a bit smaller than cited earlier.

Behavior of energy stopping

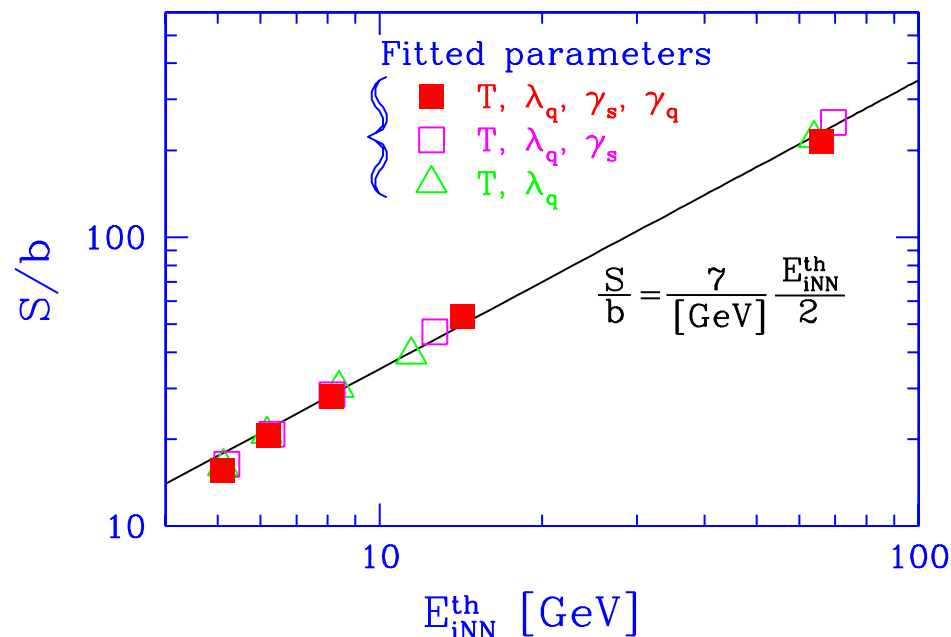


Enhanced yield of fireball intrinsic (at rest) thermal energy E_{iNN}^{th} (greater stopping) for 40 AGeV and the asymmetric S-W collision system. Relatively high RHIC result unexpected and reminiscent of PHOBOS noted identity of $y-y_p$ spectra.

DATA shown is:

SPS for 40,80,158 AGeV Pb and 200 AGeV S-W/Pb, RHIC for 65+65 AGeV Au

Entropy Production



Mechanism for parton based entropy production unknown, but appears common for SPS and RHIC.

ENTROPY PRODUCTION per unit of available energy is UNIVERSAL:

$$\frac{S}{E_i^{\text{th}}} = \frac{7}{[\text{GeV}]}$$

COMPARE SPS and RHIC STRANGENESS

STRANGENESS / FINAL STATE LIGHT QUARK PAIRS

Wróblewski ratio: In 'color string snapping' strangeness pairs $s\bar{s}$ are 4 times fewer compared to light quark pairs $q\bar{q}$. Thermal production of strangeness changes expectations.

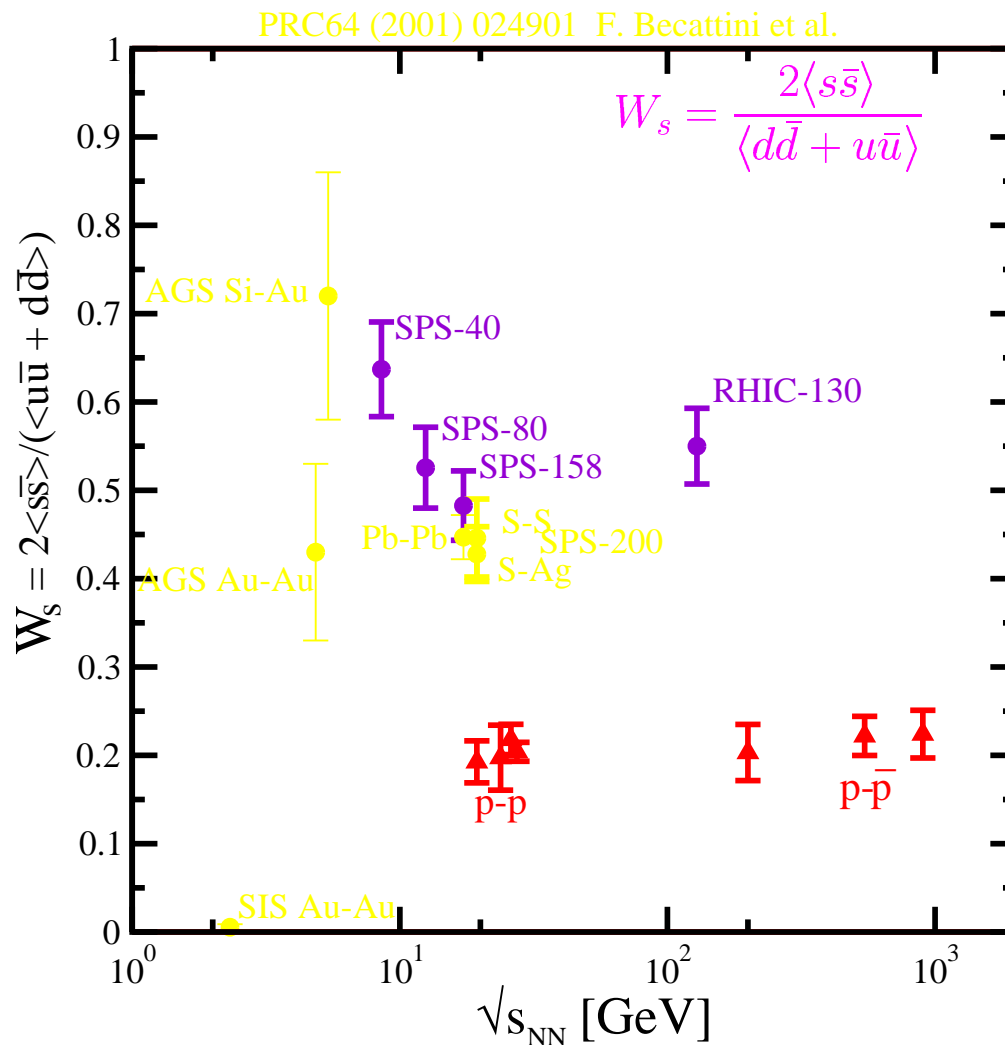
STRANGENESS / NET BARYON NUMBER

Strangeness production per thermal baryon participating in the reaction addresses the reaction energy alone, excluding variation in reaction geometry. Baryon number is conserved in hadronization. Theoretical analysis shows that true 'thermal' participants about 5-10% fewer than inferred from geometric cross section consideration.

STRANGENESS / ENTROPY CONTENT

Within QGP phase this ratio characterizes approach to chemical equilibrium of strangeness as compared to quarks and gluons. Both may increase slightly in hadronization, but are practically conserved.

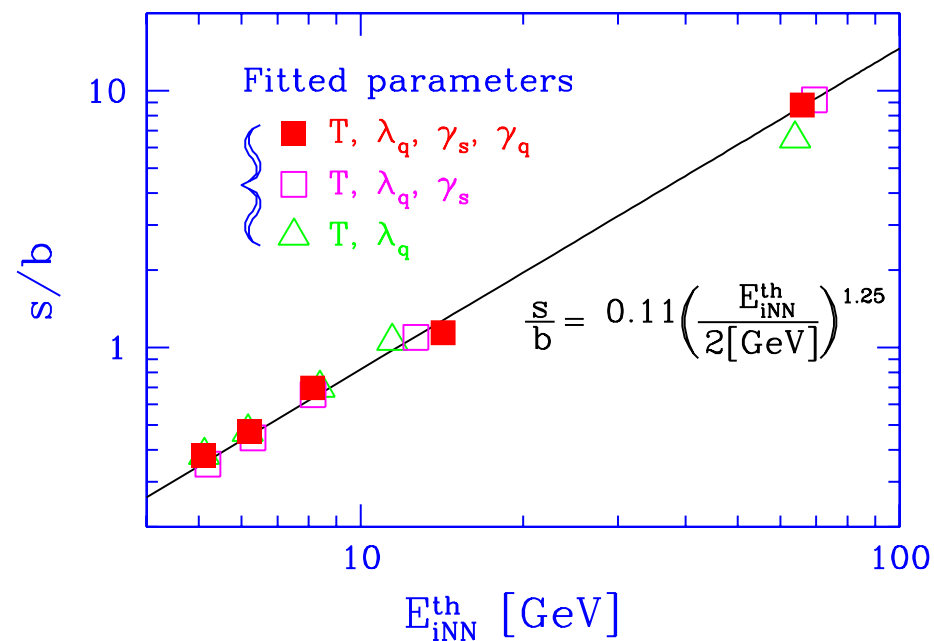
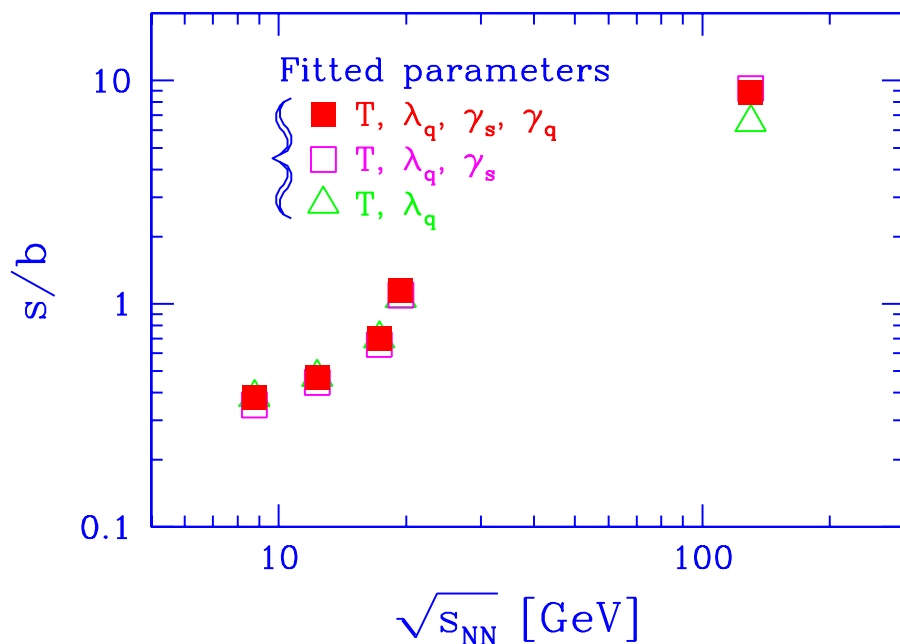
FROM SPS to RHIC: STRANGENESS vs FINAL STATE LIGHT QUARK PAIRS



Strangeness compared to light quark production: (“Wróblewski ratio”)
 only newly made s - and q -pairs are counted

Yield and \sqrt{s} dependence very different for AA and elementary reactions

FROM SPS to RHIC: STRANGENESS vs NET BARYON CONTENT

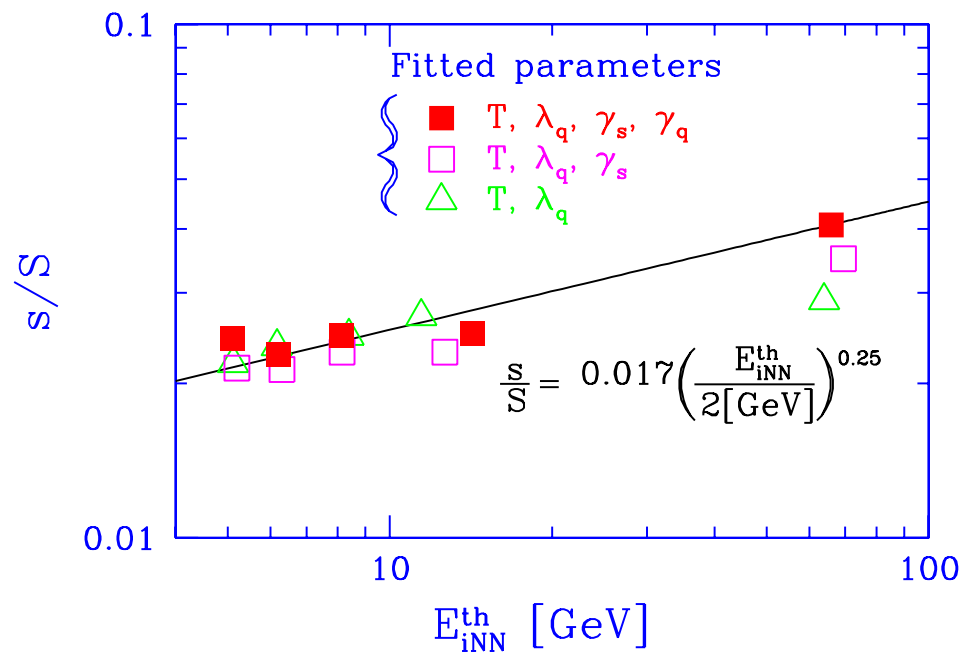
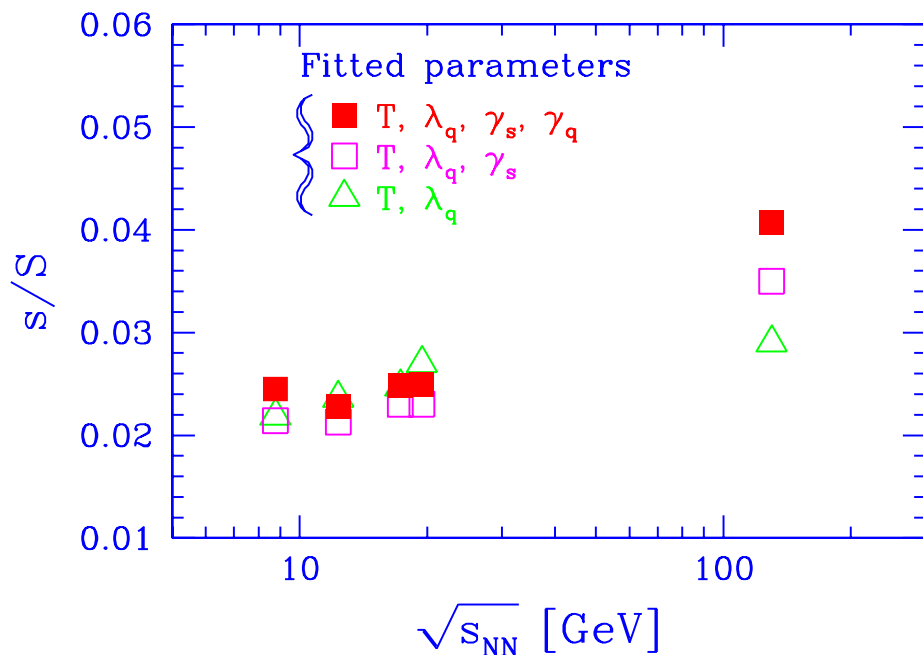


Strangeness per thermal baryon participating in the reaction grows rapidly and continuously. **Gluon based thermal production mechanism UNDERSTOOD.**

Strangeness production rises faster than entropy.

YIELD MUCH GREATER THAN IN NN-REACTIONS

FROM SPS to RHIC: STRANGENESS vs ENTROPY CONTENT



We find significant growth of strangeness per entropy from SPS to RHIC

OUTLOOK:

Anomalous strangeness yield growth below 40 GeV great opportunity for GSI:
 Longer lived deconfined phase (no explosion) at greater intrinsic energy (more stopping) cooks more strangeness?

At RHIC and soon at LHC – charm takes over – an experimental challenge

IV Quark-Gluon MATTER

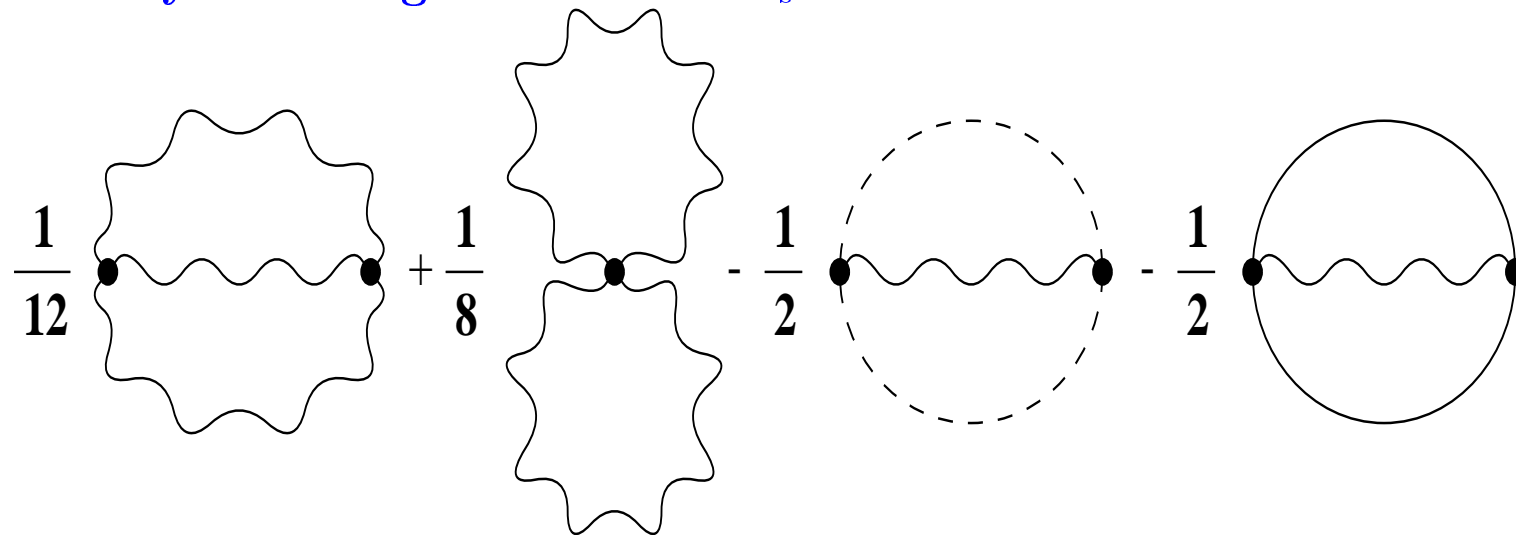
$$\ln \mathcal{Z}_{F/B}(V, \beta, \lambda, \gamma) = \pm gV \int \frac{d^3p}{(2\pi)^3} [\ln(1 \pm \gamma \lambda e^{-\beta\sqrt{p^2+m^2}}) + \ln(1 \pm \gamma \lambda^{-1} e^{-\beta\sqrt{p^2+m^2}})];$$

Boltzmann limit:

$$\ln \mathcal{Z}_{cl}(V, \beta, \lambda, \gamma) = gV \int \frac{d^3p}{(2\pi)^3} \gamma(\lambda + \lambda^{-1}) e^{-\beta\sqrt{p^2+m^2}}. \text{ for Fermi and Bose}$$

QCD perturbative interaction

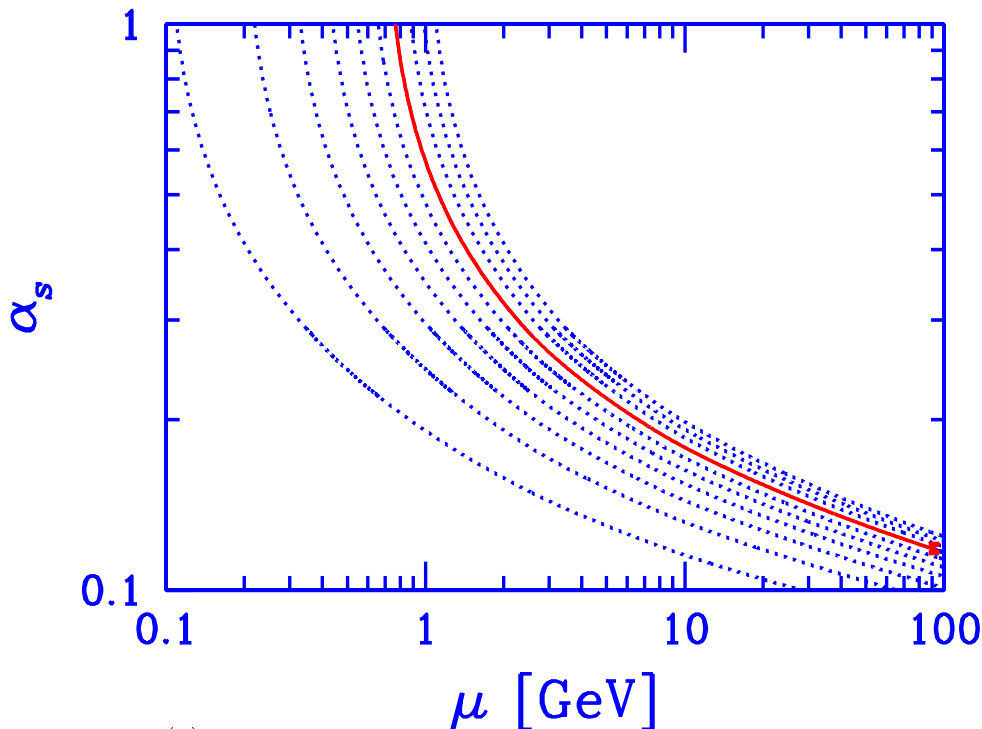
Lowest Feynman diagrams in order α_s



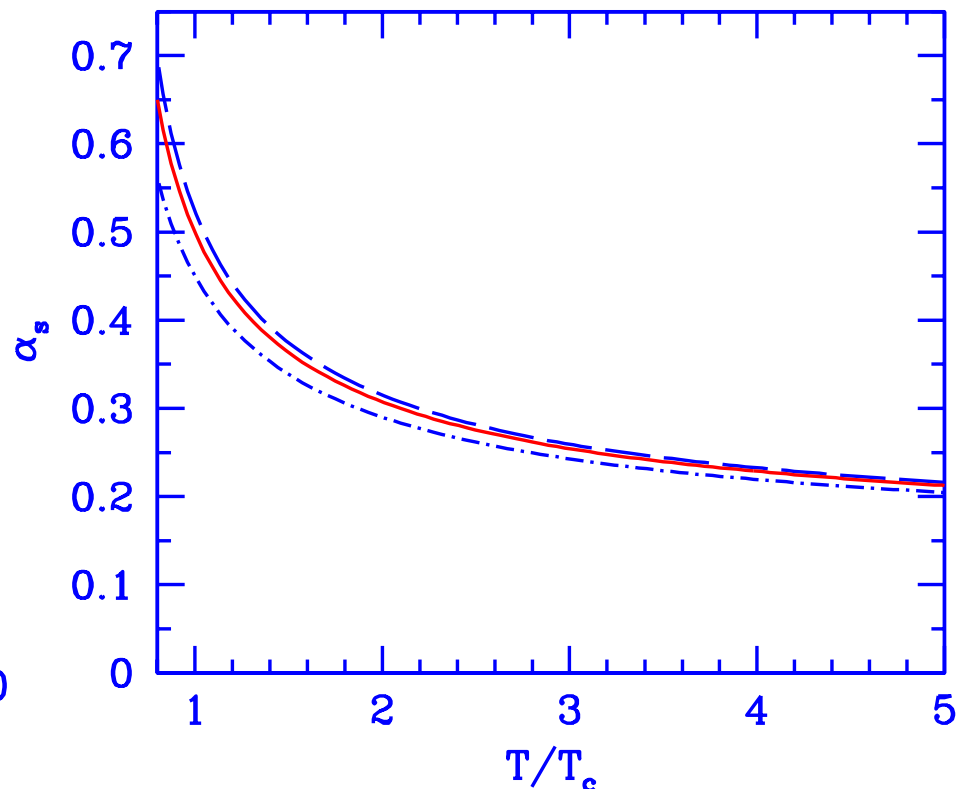
Wavy lines represent gluons, solid lines represent quarks, and dashed lines denote the ghost subtractions of non-physical degrees of freedom. Average this interaction is ATTRACTIVE and some of the many degrees of freedom freeze.

Strength of QCD coupling

the relatively small experimental value $\alpha_s(M_Z) \simeq 0.118$, experimentally established in recent years leads to “small” $\alpha_s(\mathcal{O}(\text{GeV}))$ scale:



$\alpha_s^{(4)}(\mu)$ as function of energy scale μ for a variety of initial conditions, from renormalization group.



$\alpha_s(2\pi T)$ for $T_c = 0.16 \text{ GeV}$. $\mu = 2\pi T = T/T_c$ [GeV] Dashed line: $\alpha_s(M_Z) = 0.119$; solid line = 0.118; dot-dashed = 0.1156.

For $T < 5T_c$:

$$\alpha_s(T) \simeq \frac{\alpha_s(T_c)}{1 + C \ln(T/T_c)}$$

$$\alpha_s(T_c) = 0.50_{-0.05}^{+0.03} \quad C = 0.760 \pm 0.002.$$

Perturbative QCD and QGP

$$\frac{T}{V} \ln \mathcal{Z}_{QGP} = -\mathcal{B} + \frac{8}{45\pi^2} c_1 (\pi T)^4 + \sum_{i=u,d,s} \frac{n_i}{15\pi^2} \left[\frac{7}{4} c_2 (\pi T)^4 + \frac{15}{2} c_3 \left(\mu_i^2 (\pi T)^2 + \frac{1}{2} \mu_i^4 \right) \right]$$

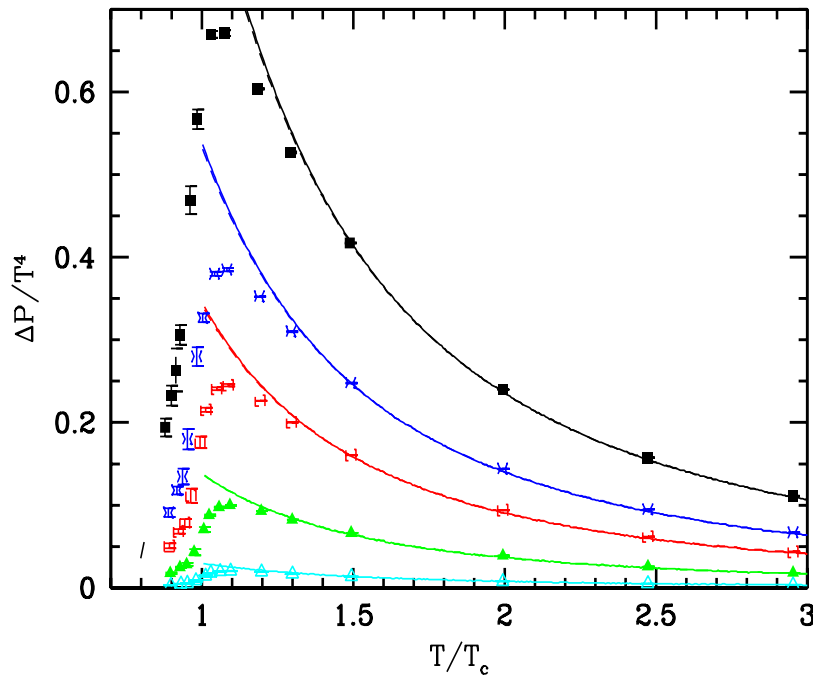
$$c_1 = 1 - \frac{15\alpha_s}{4\pi} \dots, \quad c_2 = 1 - \frac{50\alpha_s}{21\pi} \dots, \quad c_3 = 1 - \frac{2\alpha_s}{\pi} \dots$$

$$\mu_b = 3\mu_q \text{ and } \lambda_q = e^{\mu_q/T}.$$

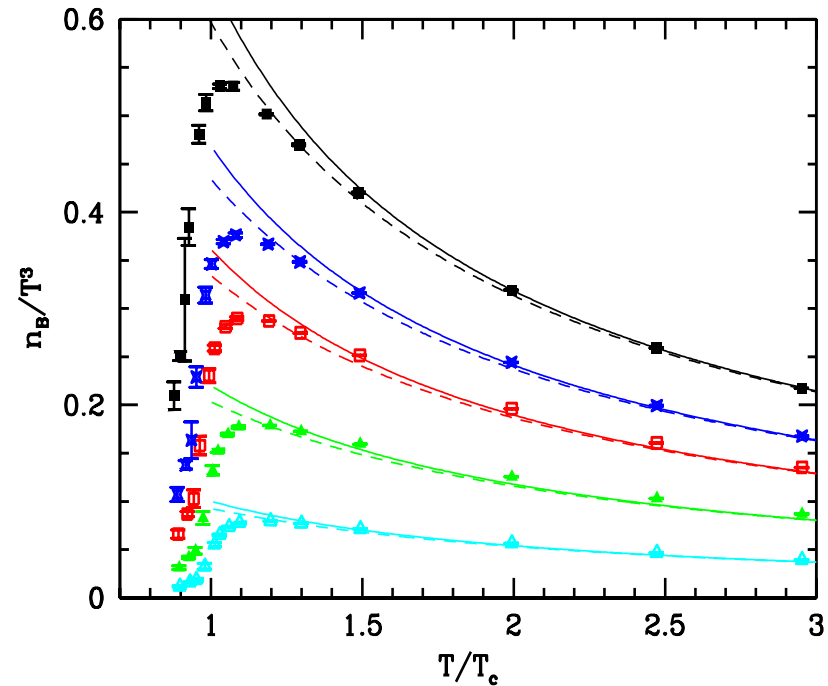
Truncating perturbative series after the first term but using the renormalization group equations yields excellent agreement with **Lattice-QCD results for both $\mu_b = 0$ and $\mu_b \neq 0$.**

Given equilibrium equations of state including phase change we can study the dynamical QGP fireball.

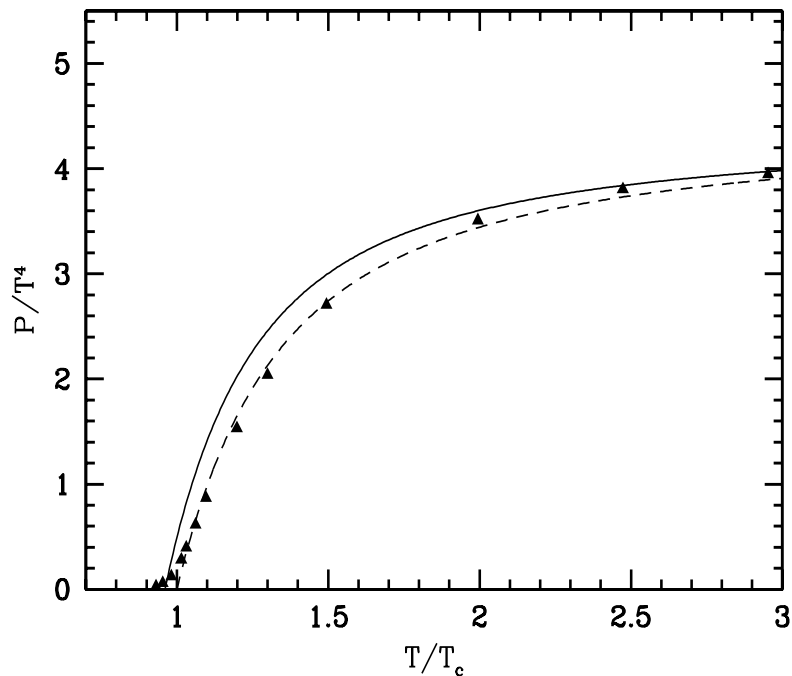
Comparison QGP-Liquid with Lattice-QCD of Fodor and Katz



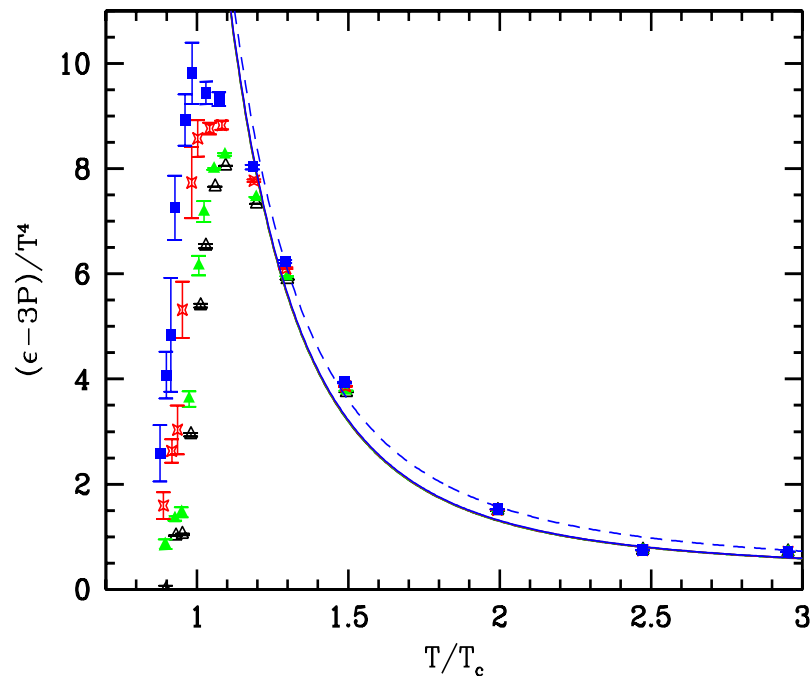
$\Delta P \equiv P(T, \mu_b) - P(T, \mu_b = 0)$ normalized by T^4 as function of T/T_c for $\mu_b = 100, 210, 330, 410$ and 530 MeV from bottom to top. Data points from Z. Fodor et al lattice work, solid lines massless liquid of quarks. Dashed (and mostly invisible) results with finite mass correction applied for $m_q = 65$ MeV as used in lattice data.



Baryon density n_B normalized by T^3 as function of T/T_c for $\mu_b = 100, 210, 330, 410$ and 530 MeV from bottom to top. Solid lines massless liquid of quarks. Dashed lines: allowance is made for $m_q = 65$ MeV as is used to obtain the lattice data.

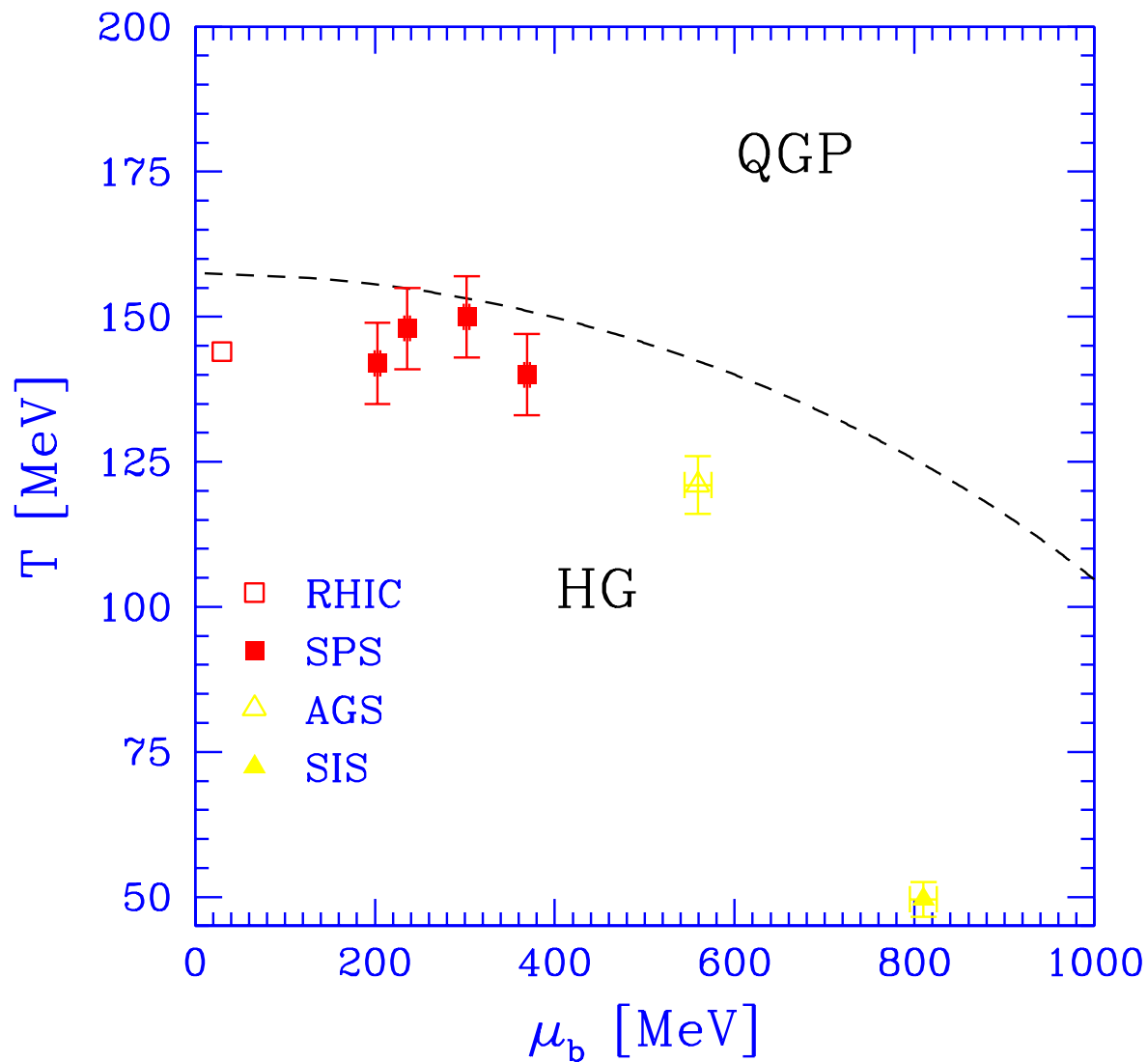


The pressure $P(T, \mu_b = 0)$ normalized by T^4 as function of T/T_c . Data points from Z. Fodor et al lattice work. Solid lines: massless gluons with $\mathcal{B} = (0.211 \text{ GeV})^4$. Dashed line allows for a finite mass $m_G = 200 \text{ MeV}$.



$(\epsilon - 3P)/T^4$ as function of T/T_c for $\mu_b = 0, 210, 410$ and 530 MeV , for $\mathcal{B} = (0.211 \text{ GeV})^4$ and $T_c = 173 \text{ MeV}$. Solid lines: massless gluons. Dashed lines: allowance is made for $m_G = 200 \text{ MeV}$. All chemical potential lines coincide within line-width.

Where are we with experimental hadron freeze-out?



Why is SPS-RHIC hadronization occurring within HG-domain?

Super-cooling of a fast expanding fireball

P and ε : local in QGP particle pressure, energy density, \vec{v} local flow velocity. The pressure component in the energy-momentum tensor:

$$T^{ij} = P\delta_{ij} + (P + \varepsilon)\frac{v_i v_j}{1 - \vec{v}^2}.$$

The rate of momentum flow vector $\vec{\mathcal{P}}$ at the surface of the fireball is obtained from the energy-stress tensor T_{kl} :

$$\vec{\mathcal{P}} \equiv \hat{\mathcal{T}} \cdot \vec{n} = P\vec{n} + (P + \varepsilon)\frac{\vec{v}_c \vec{v}_c \cdot \vec{n}}{1 - \vec{v}_c^2}.$$

The pressure and energy comprise particle and the vacuum properties: $P = P_p - \mathcal{B}$, $\varepsilon = \varepsilon_p + \mathcal{B}$. Condition $\vec{\mathcal{P}} = 0$ reads:

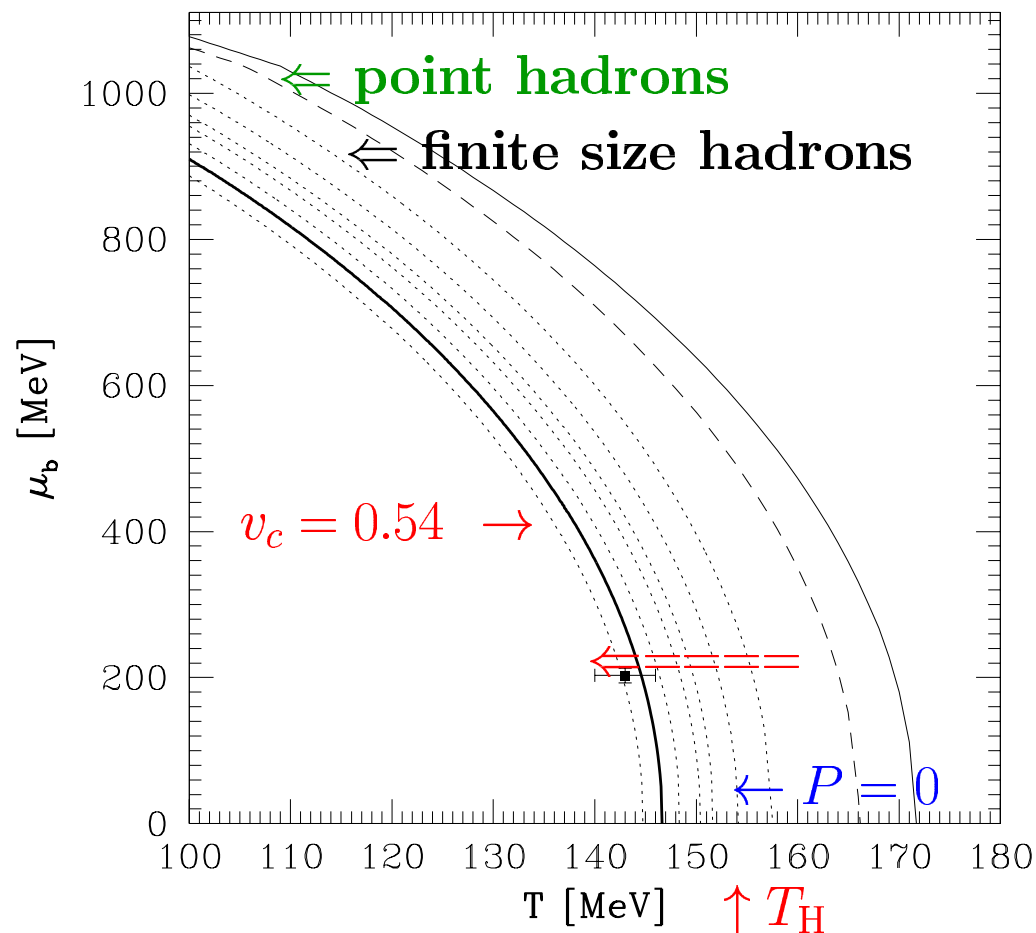
$$\mathcal{B}\vec{n} = P_p\vec{n} + (P_p + \varepsilon_p)\frac{\vec{v}_c \vec{v}_c \cdot \vec{n}}{1 - v_c^2},$$

Multiplying with \vec{n} , we find,

$$\mathcal{B} = P_p + (P_p + \varepsilon_p)\frac{\kappa v_c^2}{1 - v_c^2}, \quad \kappa = \frac{(\vec{v}_c \cdot \vec{n})^2}{v_c^2}.$$

This requires $P_p < \mathcal{B}$: QGP phase pressure P must be NEGATIVE. A fireball surface region which reaches $\mathcal{P} \rightarrow 0$ and continues to flow outward is torn apart in a rapid instability. This can ONLY arise since matter presses against the vacuum which is not subject to collective dynamics.

Phase boundary and 'wind' of flow of matter



Solid: point hadrons T_p

Dashed: finite size

Dotted: $T_c(\mu_b)|_{P_{eff}-B=0}$ for $v^2 = 0, 1/10, 1/6, 1/5, 1/4, 1/3$.

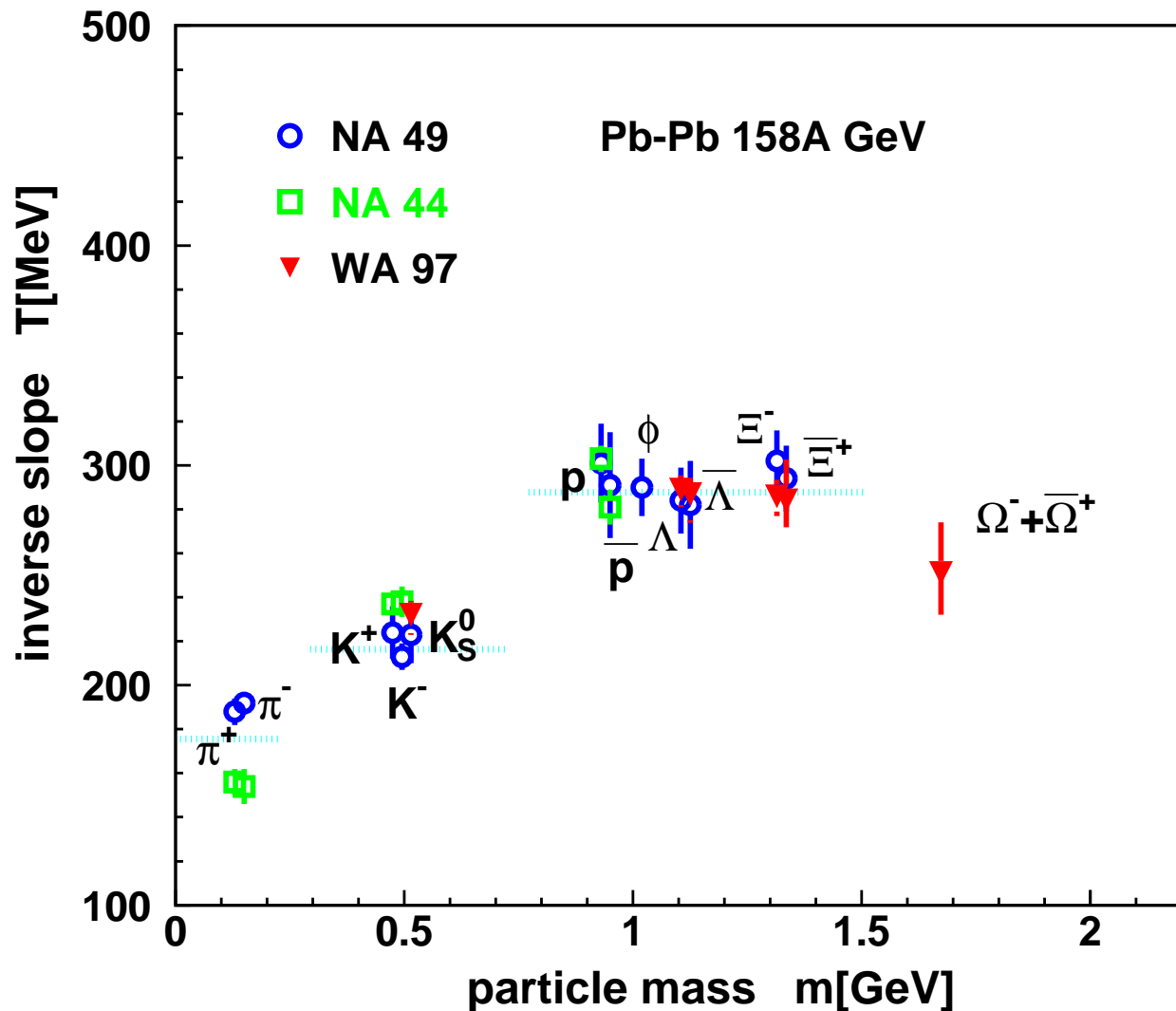
Thick solid: breakup with $v = 0.54$ ($\kappa = 0.6$)

PRL 85 (2000) 4695

**DEEP SUPERCOOLING
by 20 MeV**

$T_{Hb} = 158$ MeV Hagedorn temperature where $P = 0$, no hadron P
 $T_f \simeq 0.9T_H \simeq 143$ MeV is where supercooled QGP fireball breaks up
 equilibrium phase transformation is at $\simeq 166$.

Recall Experimental Evidence for SUDDEN HADRONIZATION



INVERSE SLOPES OF PARTICLE SPECTRA

Why are the slopes rising in value with mass?

→ EXPLOSIVE FLOW $v > 0.5c$
 More pronounced at RHIC.

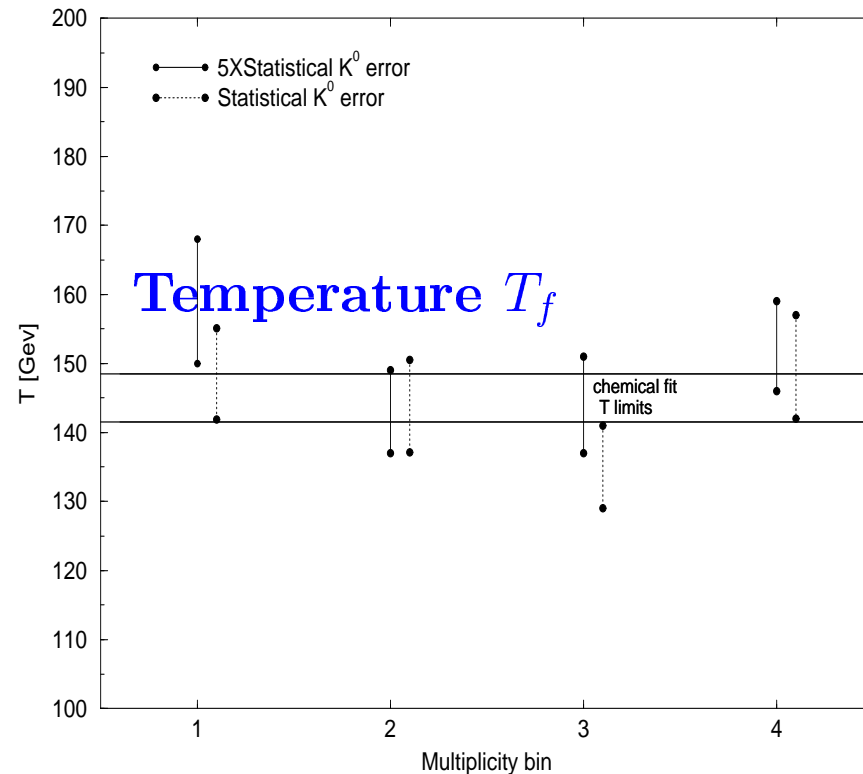
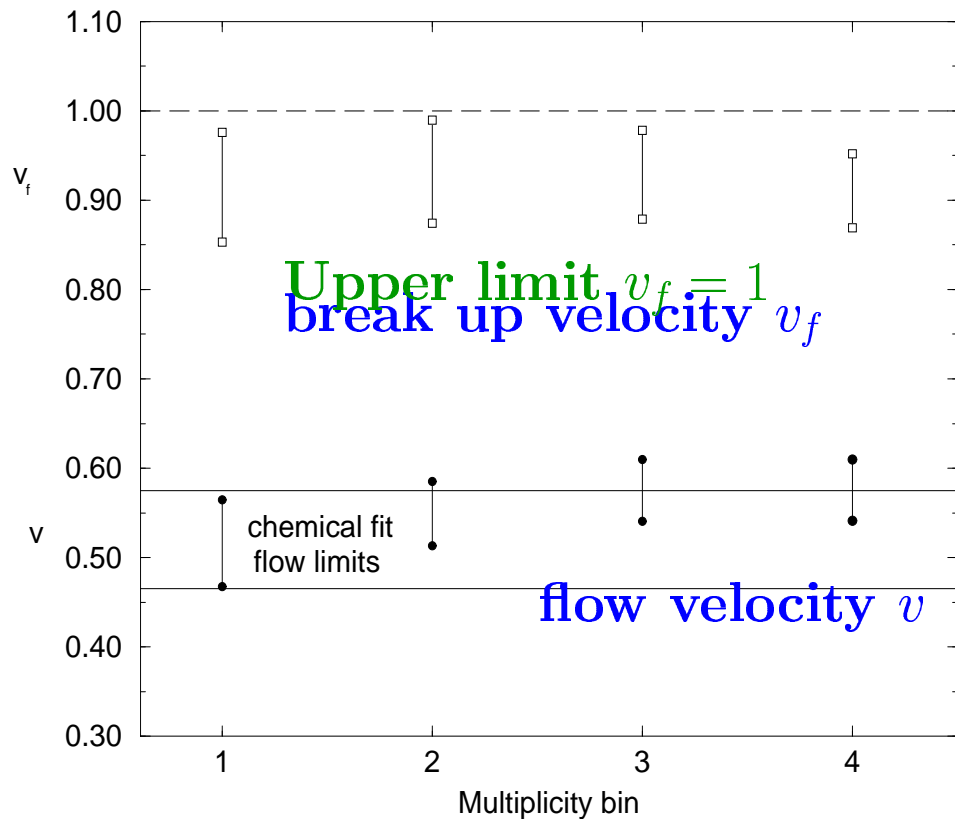
Why slopes of baryons and antibaryons precisely the same?

Same production process, and
NO REEQUILIBRATION

Diff. mass **HYPERONS** at same slope: same process, abundances include resonance decays, and
NO REEQUILIBRATION

MORE EVIDENCE FOR SUDDEN BREAKUP

CHEMICAL AND THERMAL FREEZE-OUT T, v AGREE AT SPS



5 different collision centrality bins.

by G. Torrieri

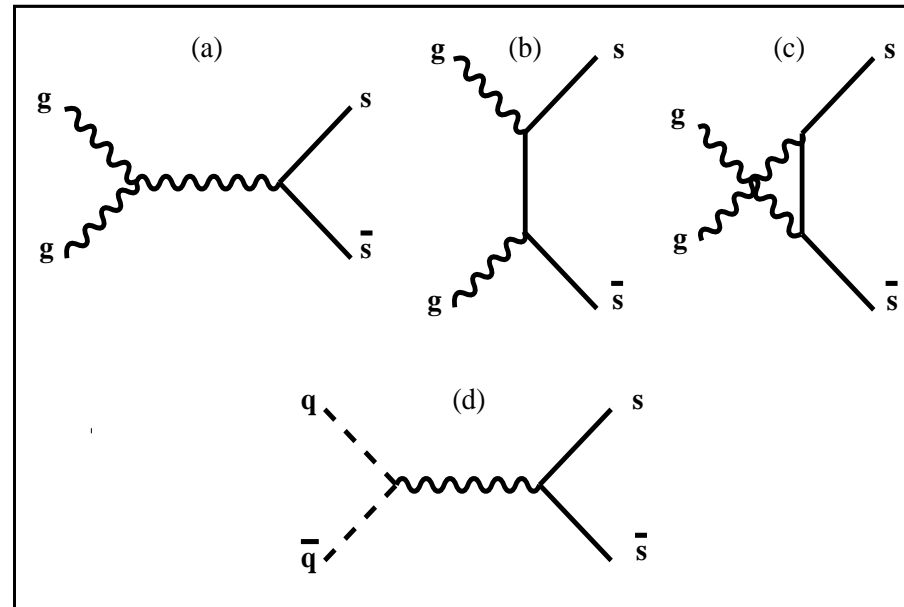
At RHIC same situation (W. Broniowski and W. Florkowski, Kraków)

FUTURE: Study of strange hadron resonances is promising to become a unique tool in exploration of hadronization dynamics.

V How the abundant strangeness can be made?

Production of strangeness in gluon fusion $GG \rightarrow s\bar{s}$

strangeness linked to gluons from QGP; *J. Rafelski and B. Müller, PRL 1981/2*



WARNING: “Thermal Production” means different things:

Here it refers to kinetic processes (see above) occurring in thermal bath of other particles.

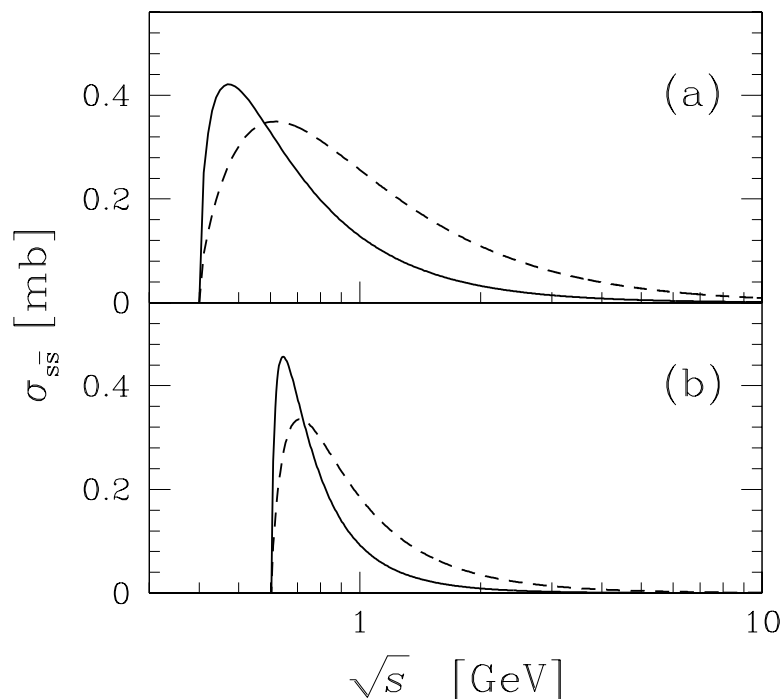
We see that “Thermal Production” is also used to describe the chemical equilibrium yield of particles.

Both usages coincide if there is enough time for kinetic processes to produce chemical equilibrium.

The generic angle averaged cross sections for (heavy) flavor s, \bar{s} production processes $g + g \rightarrow s + \bar{s}$ and $q + \bar{q} \rightarrow s + \bar{s}$, are:

$$\bar{\sigma}_{gg \rightarrow s\bar{s}}(s) = \frac{2\pi\alpha_s^2}{3s} \left[\left(1 + \frac{4m_s^2}{s} + \frac{m_s^4}{s^2} \right) \tanh^{-1}W(s) - \left(\frac{7}{8} + \frac{31m_s^2}{8s} \right) W(s) \right],$$

$$\bar{\sigma}_{q\bar{q} \rightarrow s\bar{s}}(s) = \frac{8\pi\alpha_s^2}{27s} \left(1 + \frac{2m_s^2}{s} \right) W(s). \quad W(s) = \sqrt{1 - 4m_s^2/s}$$



QGP Strangeness production cross sections:
Solid lines $q\bar{q} \rightarrow s\bar{s}$; **dashed lines** $gg \rightarrow s\bar{s}$.

a) TOP for fixed $\alpha_s = 0.6$, $m_s = 200$ MeV;
b) BOTTOM: for running $\alpha_s(\sqrt{s})$ and $m_s(\sqrt{s})$,

with $\alpha_s(M_Z) = 0.118$. $m_s(M_Z) = 90 \pm 20\%$ MeV,
 $m_s(1\text{GeV}) \simeq 2.1m_s(M_Z) \simeq 200\text{MeV}$.

Thermal average of reactions

Kinetic (momentum) equilibration is faster than chemical, use thermal particle distributions $f(\vec{p}_1, T)$ to obtain average rate:

$$\langle \sigma v_{\text{rel}} \rangle_T \equiv \frac{\int d^3 p_1 \int d^3 p_2 \sigma_{12} v_{12} f(\vec{p}_1, T) f(\vec{p}_2, T)}{\int d^3 p_1 \int d^3 p_2 f(\vec{p}_1, T) f(\vec{p}_2, T)}.$$

Invariant reaction rate in medium:

$$A^{gg \rightarrow s\bar{s}} = \frac{1}{2} \rho_g^2(t) \langle \sigma v \rangle_T^{gg \rightarrow s\bar{s}}, \quad A^{q\bar{q} \rightarrow s\bar{s}} = \rho_q(t) \rho_{\bar{q}}(t) \langle \sigma v \rangle_T^{q\bar{q} \rightarrow s\bar{s}}, \quad A^{s\bar{s} \rightarrow gg, q\bar{q}} = \rho_s(t) \rho_{\bar{s}}(t) \langle \sigma v \rangle_T^{s\bar{s} \rightarrow gg, q\bar{q}}.$$

$1/(1 + \delta_{1,2})$ introduced for two gluon processes compensates the double-counting of identical particle pairs, arising since we are summing independently both reacting particles.

This rate enters the momentum-integrated Boltzmann equation which can be written in form of current conservation with a source term

$$\partial_\mu j_s^\mu \equiv \frac{\partial \rho_s}{\partial t} + \frac{\partial \vec{v} \rho_s}{\partial \vec{x}} = A^{gg \rightarrow s\bar{s}} + A^{q\bar{q} \rightarrow s\bar{s}} - A^{s\bar{s} \rightarrow gg, q\bar{q}}$$

Strangeness density time evolution

in local restframe (\vec{v}) we have :

$$\frac{d\rho_s}{dt} = \frac{d\rho_{\bar{s}}}{dt} = \frac{1}{2}\rho_g^2(t) \langle \sigma v \rangle_T^{gg \rightarrow s\bar{s}} + \rho_q(t)\rho_{\bar{q}}(t) \langle \sigma v \rangle_T^{q\bar{q} \rightarrow s\bar{s}} - \rho_s(t)\rho_{\bar{s}}(t) \langle \sigma v \rangle_T^{s\bar{s} \rightarrow gg, q\bar{q}}$$

Evolution for s and \bar{s} identical, which allows to set $\rho_s(t) = \rho_{\bar{s}}(t)$.

Use detailed balance to simplify

$$\frac{d\rho_s}{dt} = A \left(1 - \frac{\rho_s^2(t)}{\rho_s^2(\infty)} \right), \quad A = A^{gg \rightarrow s\bar{s}} + A^{q\bar{q} \rightarrow s\bar{s}}$$

The generic solution at fixed T ($\rho \propto \tanh$) implies that in all general cases there is an exponential approach to chemical equilibrium

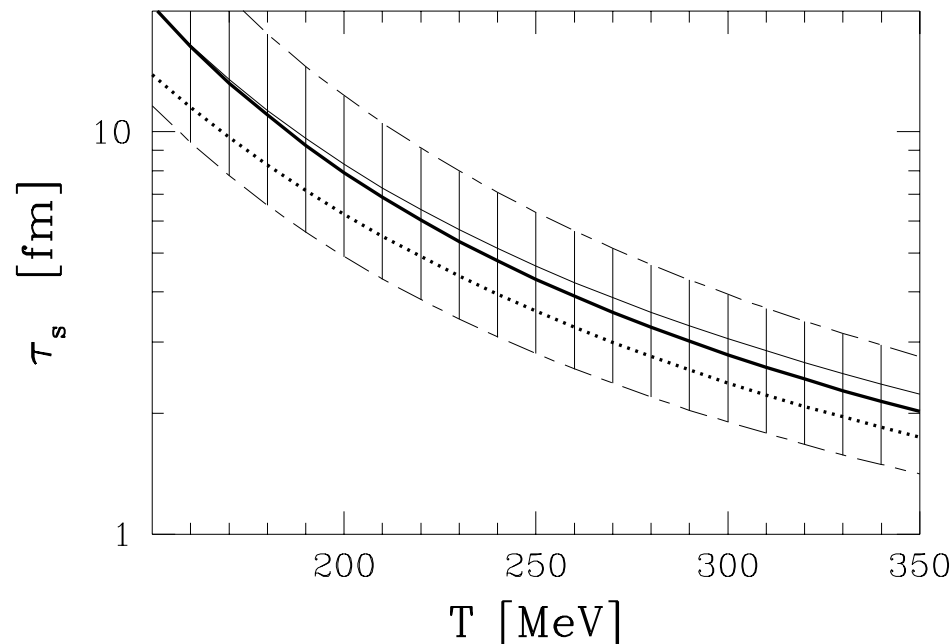
$$\frac{\rho_s(t)}{\rho_s^\infty} \rightarrow 1 - e^{-t/\tau_s}$$

with the characteristic time constant τ_s :

$$\tau_s \equiv \frac{1}{2(A^{gg \rightarrow s\bar{s}} + A^{q\bar{q} \rightarrow s\bar{s}} + \dots)} \frac{\rho_s(\infty)}{\rho_s^2(\infty)}$$

$$A^{12 \rightarrow 34} \equiv \frac{1}{1+\delta_{1,2}} \rho_1^\infty \rho_2^\infty \langle \sigma_s v_{12} \rangle_T^{12 \rightarrow 34}.$$

Characteristic time constant and γ_s -evolution

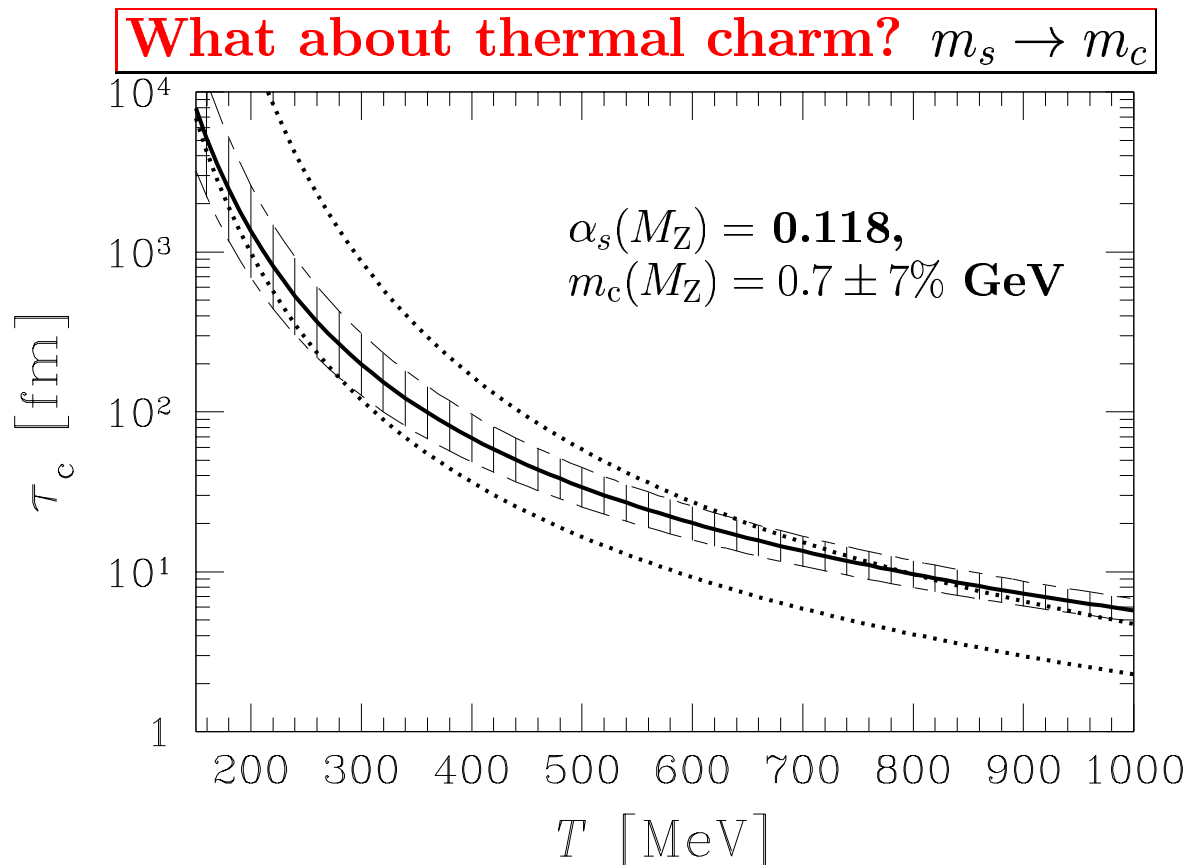


$\sigma_{\text{QCD}}^{G+G \rightarrow s\bar{s}}$ gives τ_s similar to lifespan of the plasma phase.

ENTROPY CONSERVING expansion $T^3V = \text{Const.}$ (not yet long. scaling):

$$2\tau_s \frac{dT}{dt} \left(\frac{d\gamma_s}{dT} + \frac{\gamma_s}{T} z \frac{K_1(z)}{K_2(z)} \right) = 1 - \gamma_s^2, \quad \gamma_s(t) \equiv n_s(t)/n_s^\infty, \quad z = \frac{m_s}{T}, \quad K_i : \text{Besself.}$$

compute $\gamma_s(t)$.



Thermal charm production is of relevance only for $T \rightarrow m_c(1 \text{ GeV}) \simeq 1.5 \text{ GeV}$, probably not accessible.

OUTLOOK: Charm is produced abundantly in first parton collisions. **Benchmark:** 10 $c\bar{c}$ pairs in central Au–Au at RHIC-200; and 200 $c\bar{c}$ pairs in central Pb–Pb LHC-5500 reactions (R.L. Thews). This yield is greater than the expected equilibrium yield at hadronization of QGP. Charm hadronization probes of deconfinement.

FINAL REMARKS

Strangeness at CERN-SPS and BNL-RHIC is a well developed tool

allowing to study

Deconfinement and QGP-Hadronization

Systematic study of strangeness offers a fingerprint a new state of matter

Outlook:

search for the onset of deconfinement

at RHIC study of hadronization dynamics with the help of strange resonances

FUTURE:

as instrumentation improves charm replaces strangeness at RHIC and LHC

as the tool in the study of deconfined matter

APOLOGIES: I believe to be a better physicist than historian – please accept my apologies for any historical and/or citation omissions.

J. Rafelski